



## New insights on the adsorption, thermal decomposition and reduction of $\text{NO}_x$ over Pt- and Ba-based catalysts



L. Castoldi<sup>a</sup>, R. Matarrese<sup>a</sup>, S. Morandi<sup>b</sup>, L. Righini<sup>a</sup>, L. Lietti<sup>a,\*</sup>

<sup>a</sup> Dipartimento di Energia, Laboratory of Catalysis and Catalytic Processes and NEMAS, Centre of Excellence, Politecnico di Milano, Via La Masa 34, 20156 Milano, Italy

<sup>b</sup> Dipartimento di Chimica and NIS, Inter-departmental Center, Università di Torino, Via P. Giuria 7, 10125 Torino, Italy

### ARTICLE INFO

#### Keywords:

$\text{NO}_x$  adsorption  
Nitrite and nitrate formation  
 $\text{PtBa/Al}_2\text{O}_3$   
 $\text{Pt/Al}_2\text{O}_3 + \text{Ba/Al}_2\text{O}_3$  mechanical mixture  
 $\text{NO}_x$  thermal decomposition

### ABSTRACT

In this study mechanistic aspects related to the adsorption of  $\text{NO}_x$  over alumina-supported Pt, Ba and PtBa catalysts are deepened, that are of interest for  $\text{NO}_x$  Storage-Reduction (NSR) catalysts and other applications involving the adsorption of  $\text{NO}_x$  (e.g. Passive  $\text{NO}_x$  Adsorbers, PNAs).  $\text{NO}_x$  adsorption is investigated at low and high temperatures (150 °C and 350 °C, respectively); the thermal decomposition and the reactivity with  $\text{H}_2$  of the adsorbed species is also addressed. By coupling FT-IR spectroscopy and microreactor studies, new insights on the adsorption, decomposition and reactivity of the stored  $\text{NO}_x$  are derived. In particular it is found that at 150 °C nitrites are formed on all surfaces when starting from  $\text{NO}/\text{O}_2$ ; different species are formed onto the different storage sites (Ba vs. Al) that can be distinguished spectroscopically. Different routes for the storage of nitrites are highlighted, i.e. direct oxidative NO uptake and nitrite formation involving  $\text{NO}_2$  produced by oxidation of NO. Clear and novel evidence is herein provided that the direct NO oxidative uptake is much faster than the route involving the NO to  $\text{NO}_2$  oxidation. Both routes are catalyzed by Pt, although Ba is also able to store nitrites; the role of the interaction between Pt and the storage sites is discussed. When the  $\text{NO}_x$  storage is carried out at higher temperatures (350 °C), both routes are greatly favored although nitrites can hardly be observed being readily transformed into nitrates. Besides  $\text{NO}_2$  is also formed in significant amounts that may participate to the formation of nitrites/nitrates adspecies following a  $\text{NO}_2$  disproportion pathway for which clear and new spectroscopic evidences are herein provided.

The adsorbed species (nitrites or nitrates) start to decompose above the adsorption temperature, i.e. 150 °C and 350 °C, respectively. In the presence of Pt, the decomposition of the stored nitrites leads to the formation of nitrates and NO due to the occurrence of a nitrite disproportion reaction. The formed nitrates show high thermal stability and decompose only at high temperatures, thus making these systems unappropriate for PNA applications. In the presence of a reductant, Pt catalyzes the reduction of the stored  $\text{NO}_x$  at much lower temperatures than the adsorption; the role of the interaction between Pt and the storage sites on this step is herein discussed.

### 1. Introduction

According to the European Environmental Agency (EEA), air pollution has a significant impact on human health, particularly in urban areas. In Europe, this has considerable economic impacts, cutting lives short, increasing medical costs and reducing productivity through working days lost across the economy.

Europe's most problematic pollutants in terms of harm to human health are Particulate Matter (PM), ground-level  $\text{O}_3$  and  $\text{NO}_2$ . Concerning  $\text{NO}_2$ , estimates indicate that in 2012 the impact of exposure to  $\text{NO}_2$  (long-term exposure) concentrations on the population resulted in around 72000 premature deaths in the EU28. Although emissions of the main air pollutants in Europe have declined since 1990, resulting in

generally improved air quality across the region, in a few sectors emissions have not been sufficiently reduced to meet air quality standards, or have even been increased. For example, road transport, and in particular diesel engines, still remains one of the major responsible in many urban areas for the emissions of nitrogen oxides ( $\text{NO}_x$ ), that are the source of  $\text{NO}_2$  [1].

For these reasons, current and upcoming worldwide environmental regulation (e.g. Euro 6 and 7, US EPA Tier III and California LEV III) requires vehicles with extremely reduced  $\text{NO}_x$  emissions. Current technologies for  $\text{NO}_x$  abatement from diesel engines are based on the  $\text{NH}_3$  selective catalytic reduction (SCR) technology, or on the  $\text{NO}_x$ -Storage Reduction (NSR) technique, also referred as Lean  $\text{NO}_x$  traps (LNT) [2,3]. In the SCR technology the  $\text{NO}_x$  reduction is based on the

\* Corresponding author.

E-mail address: [luca.lietti@polimi.it](mailto:luca.lietti@polimi.it) (L. Lietti).

use of Cu/or Fe/zeolite catalysts coupled with an urea injection system. This is an effective approach for treating the  $\text{NO}_x$  emissions from diesel engines once the exhaust temperatures are above 200 °C [4]. Such temperature limit is due to need of avoiding the incomplete hydrolysis of urea; therefore,  $\text{NO}_x$  produced during the vehicle cold start period before the SCR catalyst reaches the operating temperatures [4] are not reduced.

At variance, the NSR catalytic technology has been introduced in the '90 s by Toyota Motor Company and is based on sequential  $\text{NO}_x$  adsorption/reduction cycles [2,3,5,6]. In fact, in these systems  $\text{NO}_x$  are stored on the catalyst during the lean operation of the engine; the stored  $\text{NO}_x$  are then reduced to  $\text{N}_2$  (and other by-products like  $\text{N}_2\text{O}$  and  $\text{NH}_3$ ) during periodic rich purges. Accordingly, a LNT catalyst comprises sites for  $\text{NO}_x$  sorption (alkali metal or alkaline earth metal compounds like K and/or Ba, or Ce) [2,6,7] and sites for  $\text{NO}_x$  oxidation/reduction, generally noble metals like Pt and/or Rh, Pd [2]. This technology is effective for the reduction of  $\text{NO}_x$  emissions although it may lead to a slight increase of the fuel consumption (fuel penalty) due to the rich excursions; besides the catalysts show poor reactivity below 150–200 °C. To avoid  $\text{NH}_3$  emissions (that may be formed during the rich excursions) and to increase the  $\text{NO}_x$  reduction efficiency, hybrid NSR + SCR systems have also been proposed [8–11].

To reduce cold-start  $\text{NO}_x$  emissions an attractive option is the use of the so-called Passive  $\text{NO}_x$  Adsorber (PNA) [12]. This technology consists of an upstream trap that stores  $\text{NO}_x$  during the cold start period ( $T_{\text{exhaust}} < 180\text{--}200$  °C); the stored  $\text{NO}_x$  are released when the downstream  $\text{NO}_x$  abatement catalyst reaches a suitable operating temperature. The DOC catalyst placed upstream the NSR/SCR system may contribute to  $\text{NO}_x$  adsorption at low temperatures; however specifically designed noble-metal doped zeolitic materials [13–15] have been suggested, along with  $\text{Al}_2\text{O}_3$ - or  $\text{CeO}_2$ -supported Pt/Pd and Ag/ $\text{Al}_2\text{O}_3$  catalysts. Notably, NSR systems may trap significant amounts of  $\text{NO}_x$  at low temperatures as well, being their reactivity during cyclic operation limited by the onset temperature for the reduction of the stored  $\text{NO}_x$ .

On these bases, a better understanding of the mechanisms involved in the adsorption of  $\text{NO}_x$  over alumina-supported catalysts, and on the thermal decomposition and reactivity of the stored  $\text{NO}_x$  is noteworthy. This has motivated our study where alumina supported catalytic systems have been selected in view of their potential interest in NSR, DOC and PNA applications. In particular, in this study we have focused the attention on the interaction of  $\text{NO}_x$  (starting from  $\text{NO}/\text{O}_2$  mixtures) with different alumina-supported model catalysts, i.e. a Pt/ $\text{Al}_2\text{O}_3$  sample (representative of a DOC system), a Ba-doped alumina used as storage material and a Pt-Ba/ $\text{Al}_2\text{O}_3$  LNT catalyst sample. A Pt/ $\text{Al}_2\text{O}_3$  + Ba/ $\text{Al}_2\text{O}_3$  physical mixture has also been considered to provide further indications on the role of the Pt-Ba interaction on the adsorption of  $\text{NO}_x$  and on their thermal decomposition and reactivity. The adsorption of NO in the presence of oxygen has been investigated at low and high temperatures (150 °C and 350 °C, respectively) by coupling flow microreactor experiments and *operando* FT-IR spectroscopy. Then, the thermal decomposition of the  $\text{NO}_x$  species stored at 150 °C and 350 °C and their reactivity towards  $\text{H}_2$  (selected as reducing agent) has been investigated by temperature programmed desorption (TPD) and isothermal reduction, respectively, coupled with FT-IR spectroscopy. Mechanistic details on the adsorption of  $\text{NO}_x$  have been further disclosed by investigating the adsorption of  $\text{NO}_2$  and of  $\text{NO}/\text{NO}_2$  mixtures over selected samples. Therefore new pieces of evidence have been provided on the complex interplay among the various catalyst components (alumina support, storage element and noble metal) involved in the adsorption, thermal decomposition and reduction of the stored  $\text{NO}_x$  species. The role of the Pt/Ba interaction on these functionalities has also been investigated.

Experiments have been performed in the absence of water, but the effect of this species has been investigated as well in selected experiments or recalled from previous literature data. Besides, freshly prepared catalyst samples have been used. As shown by several

investigations (see e.g. [16,17]), it is recognized that hydrothermal aging leads to sintering of the precious metal, thus deteriorating the Pt/Ba interface. This results in a decrease of the catalytic performances due to changes in the efficiency of the catalytic pathways involved in the functioning of the LNT catalysts (NO oxidation,  $\text{NO}_x$  storage,  $\text{NO}_x$  release,  $\text{NO}_x$  reduction), but not in different reaction mechanisms. Accordingly the obtained results may contribute to the understanding of the behavior of  $\text{NO}_x$  storage materials.

## 2. Experimental

### 2.1. Catalyst preparation and characterization

All catalyst samples have been prepared according to the Toyota recipes [18]. In particular Pt/ $\text{Al}_2\text{O}_3$  (1/100 w/w) and Ba/ $\text{Al}_2\text{O}_3$  (20/100 w/w) catalysts have been prepared by incipient wetness impregnation, starting from a  $\gamma\text{-Al}_2\text{O}_3$  support (Versal 250 from UOP, calcined at 700 °C) and aqueous solutions of dinitro-diammine platinum (Strem Chemicals, 5% Pt in ammonium hydroxide) and of barium acetate (Aldrich, 99%) for Pt and Ba, respectively. After impregnation, the samples have been dried at 80 °C overnight and calcined at 500 °C for 5 h. The ternary Pt-Ba/ $\text{Al}_2\text{O}_3$  (1/20/100 w/w) catalyst sample has been prepared with the same procedure. Pt has been incorporated as first and then Ba; after each impregnation step the sample has been dried at 80 °C overnight and calcined at 500 °C for 5 h. Freshly calcined catalyst samples have been used in this study.

The specific surface area of the Pt/ $\text{Al}_2\text{O}_3$ , Ba/ $\text{Al}_2\text{O}_3$  and Pt-Ba/ $\text{Al}_2\text{O}_3$  samples (measured by BET method) is 194  $\text{m}^2\text{g}^{-1}$ , 136  $\text{m}^2\text{g}^{-1}$  and 160  $\text{m}^2\text{g}^{-1}$ , respectively. The Pt dispersion in the Pt/ $\text{Al}_2\text{O}_3$  and Pt-Ba/ $\text{Al}_2\text{O}_3$  samples, estimated as reported in [19], is near 90% and 52%, respectively. The ternary catalyst exhibits a lower Pt dispersion than the binary Pt/ $\text{Al}_2\text{O}_3$  possibly due to the masking of the Pt crystallites by the Ba component [20].

XRD diffraction analysis showed in all cases peaks related to microcrystalline  $\gamma\text{-Al}_2\text{O}_3$ . Orthorhombic and monoclinic  $\text{BaCO}_3$  (traces) have also been detected in the Ba-containing samples. Further details about preparation, morphology and further characterization of the catalyst can be found elsewhere [21].

### 2.2. Catalytic tests

The catalytic tests have been performed by using 60 mg of a single catalyst powder (70–100  $\mu\text{m}$ ) or 60 + 60 mg in the case of the physical mixture, in order to operate in all cases with the same amount of Pt and Ba in the reactor. The latter consists of a quartz tube (7 mm I.D.) heated by an electric furnace. Gases were fed to the reactor by means of mass-flow controllers, by using calibrated gas cylinders (NO in He,  $\text{NO}_2$  in He,  $\text{O}_2$  in He,  $\text{H}_2$  in He) also containing Ar as inert tracer. A total flow rate of 100 cc/min (at 0 °C and 1 atm) has always been used during all experiments.

The reactor products have been on-line monitored in continuous by a mass spectrometer (Thermostar 200, Pfeiffer Vacuum) and an UV- $\text{NO}_x$  analyser (LIMAS 11HW, ABB) and with punctual analyses by a micro-gas chromatograph (A3000, Agilent). By combining the independent analyses of the three instruments it is possible to ensure an accurate quantitative analysis of the gases exiting the reactor.

The  $\text{NO}_x$  storage has been carried out at low and high temperature (150 °C and 350 °C, respectively) starting from NO (1000 ppm) +  $\text{O}_2$  (3% v/v) in He. In a typical experiment, NO is added in a stepwise manner to the flowing He +  $\text{O}_2$  mixture, while monitoring the reactor outlet. When steady-state conditions are reached, the NO concentration is decreased back to zero and the catalyst has been purged with He at the same temperature to remove weakly adsorbed species.

The thermal decomposition of the adsorbed species has been investigated by temperature programmed desorption (TPD) after adsorption followed by He purge and cooling down to 50 °C, followed by

heating to 500 °C (heating rate 10 °C/min) under He.

When the effect of water in the feed has been investigated, 1% H<sub>2</sub>O (v/v) has been added to the feed stream.

The reactivity of stored NO<sub>x</sub> towards H<sub>2</sub> has been studied after NO<sub>x</sub> storage by admitting 2000 ppm of H<sub>2</sub> to the reactor at constant temperature (150 °C and 350 °C), with an inert purge in between.

Prior to any catalytic run the catalysts have been conditioned through NO<sub>x</sub> adsorption/reduction cycles (typically 3–4 cycles) at 350 °C starting from NO/O<sub>2</sub> and H<sub>2</sub> mixtures or by TPD in order to remove Ba(CO<sub>3</sub>)<sub>2</sub> species from the surface.

### 2.3. FT-IR surface analysis

The evolution of the surface species has been also analyzed by FT-IR spectroscopy performed under *operando* conditions. Absorption/transmission IR spectra were run on a Perkin-Elmer FT-IR System 2000 spectrophotometer equipped with a Hg-Cd-Te cryo-detector, working in the range of wavenumbers 7200–580 cm<sup>-1</sup> at a resolution of 2 cm<sup>-1</sup>. For IR analysis powder samples were compressed in self-supporting discs (10 mg cm<sup>-2</sup> for Pt/Al<sub>2</sub>O<sub>3</sub> and Ba/Al<sub>2</sub>O<sub>3</sub>, 20 mg cm<sup>-2</sup> for the 1:1 physical mixture) and placed in a commercial IR reactor cell (Aabspec) under a flow of 50 Ncc/min. The NO<sub>x</sub> storage has been carried out at 150 °C and 350 °C starting from NO (1000 ppm) + O<sub>2</sub> (6% v/v) in He, followed by a He purge at the storage temperature to remove weakly adsorbed species. During the storage, the spectra are recorded at increasing time on stream.

After the storage and purging phase, temperature programmed desorption (TPD) has been performed by heating from 150 °C or 350 °C up to 500 °C (heating rate 10 °C/min) under He flow. During the TPD, the spectra are recorded every 2 min. As in the case of catalytic tests, prior to any IR run the catalysts have been conditioned through adsorption/reduction cycles (typically 3–4 cycles) at 350 °C starting from NO/O<sub>2</sub> and H<sub>2</sub> mixtures or by TPD in order to remove Ba(CO<sub>3</sub>)<sub>2</sub> species from the surface as much as possible.

The spectra are reported as difference spectra in the figures. The background spectrum is always that obtained after the conditioning treatment just described.

Like in the case of the catalytic tests, when the effect of water in the feed has been investigated, 1% H<sub>2</sub>O (v/v) has been added to the feed gas.

## 3. Results and discussion

### 3.1. Surface species involved in the adsorption of NO/O<sub>2</sub>

#### 3.1.1. Adsorption at 150 °C

Fig. 1 shows the results (gas phase analysis and FT-IR) of the storage phase carried out at 150 °C over Ba/Al<sub>2</sub>O<sub>3</sub> and Pt/Al<sub>2</sub>O<sub>3</sub> catalysts.

Upon NO admission to Ba/Al<sub>2</sub>O<sub>3</sub> catalyst (Fig. 1A), the NO concentration rapidly increases reaching the inlet NO concentration. No NO<sub>2</sub> is detected at the reactor outlet, as expected in view of the poor activity of Ba oxide in the oxidation of NO to NO<sub>2</sub>. After NO shutoff a small tail in the NO concentration is observed, suggesting that the adsorbed species are quite stable. The quantitative analysis indicates a limited NO<sub>x</sub> adsorption at steady-state (0.12 mmol/g<sub>cat</sub>); a small decrease in the amounts of stored NO<sub>x</sub> is observed after NO and O<sub>2</sub> shutoff (see Fig. 2A).

Surface FT-IR analysis recorded in this case (Fig. 1B) shows the formation of mainly ionic nitrites on Ba sites, characterized by the bands at 1215 cm<sup>-1</sup> and 1360 cm<sup>-1</sup> related to  $\nu_{\text{asym}}(\text{NO}_2)$  and  $\nu_{\text{sym}}(\text{NO}_2)$  modes, respectively. The concentration of such species increases with time on stream. Lower amounts of bidentate nitrates (1565 cm<sup>-1</sup>,  $\nu(\text{N}=\text{O})$  mode) are also formed.

Different features are observed in the case of Pt/Al<sub>2</sub>O<sub>3</sub> catalyst. From the gas phase analysis (Fig. 1C) it appears that NO is immediately observed at the reactor outlet, but a knee is apparent in the outlet NO

concentration trace. NO<sub>2</sub> is also formed in this case, near 20 ppm at steady state. Note that NO oxidation is apparent due to the presence of Pt sites. Higher amounts of NO<sub>x</sub> are stored in this case (0.26 mmol/g<sub>cat</sub>, see Fig. 2A); however, after NO and O<sub>2</sub> shutoff a pronounced tail in the NO concentration is observed, leading to a decrease in the amounts of the NO<sub>x</sub> adsorbed species (see Fig. 2A). The FT-IR spectra reported in Fig. 1D show that over the Pt/Al<sub>2</sub>O<sub>3</sub> catalyst nitrites are mainly formed, both ionic ( $\nu_{\text{asym}}(\text{NO}_2)$  and  $\nu_{\text{sym}}(\text{NO}_2)$  modes at 1230 and 1316 cm<sup>-1</sup>, respectively) and linear ( $\nu(\text{N}=\text{O})$  and  $\nu(\text{N}=\text{O})$  modes at 1077 and 1550 cm<sup>-1</sup>, respectively). Much lower amounts of bidentate nitrates ( $\nu(\text{N}=\text{O})$  modes at 1616 and 1467 cm<sup>-1</sup>) are also observed. Worth to note that the ionic nitrite bands in the Pt/Al<sub>2</sub>O<sub>3</sub> spectra are much narrower than those observed in the case of the Ba/Al<sub>2</sub>O<sub>3</sub> sample, suggesting a lower heterogeneity of nitrite species on Pt/Al<sub>2</sub>O<sub>3</sub> than on the Ba/Al<sub>2</sub>O<sub>3</sub> sample.

The storage of NO/O<sub>2</sub> has been carried out at 150 °C also over Pt-Ba/Al<sub>2</sub>O<sub>3</sub> ternary catalyst and over the Pt/Al<sub>2</sub>O<sub>3</sub> + Ba/Al<sub>2</sub>O<sub>3</sub> physical mixture as well and the results are reported in Fig. 3A–B and C–D respectively.

In the case of NO/O<sub>2</sub> adsorption on Pt-Ba/Al<sub>2</sub>O<sub>3</sub> (Fig. 3A), NO is detected at the reactor exit with a delay of 60 s, then its concentration increases with time. The formation of NO<sub>2</sub> is also observed after more than 500 s from the beginning of the storage phase; at steady-state the NO<sub>2</sub> concentration is near 15 ppm, i.e. a slightly lower value than for the Pt/Al<sub>2</sub>O<sub>3</sub> sample. As shown in Fig. 3B, the NO adsorption results in the formation of ionic nitrites with characteristic bands at 1360 cm<sup>-1</sup> [ $\nu_{\text{sym}}(\text{NO}_2)$ ] and at 1215 cm<sup>-1</sup> [ $\nu_{\text{asym}}(\text{NO}_2)$ ]; these species grow during storage. A small band at 1546 cm<sup>-1</sup> is also observed, assigned to the  $\nu(\text{N}=\text{O})$  mode of bidentate nitrates [22]. Hence it is concluded that at low temperature (150 °C) NO<sub>x</sub> are stored mainly in the form of nitrites, according to spectroscopic data in the early LNT literature [22]. Adsorbed amounts of NO<sub>x</sub> near 0.494 mmol/g<sub>cat</sub> have been estimated up to NO<sub>x</sub> catalyst saturation in this case (see Fig. 2A), in line with those reported in literature for typical LNT catalytic system [19,23]. Like in the previous case, after NO and O<sub>2</sub> shutoff, a tail is observed in NO<sub>x</sub> concentration, leading to a decrease of the stored NO<sub>x</sub>.

Finally, in the case of the Pt/Al<sub>2</sub>O<sub>3</sub> + Ba/Al<sub>2</sub>O<sub>3</sub> physical mixture at 150 °C the NO<sub>x</sub> breakthrough is null (Fig. 3C, gas phase analysis). The formation of NO<sub>2</sub> is also limited (near 45 ppm), although slightly higher than that of both Pt-Ba/Al<sub>2</sub>O<sub>3</sub> and Pt/Al<sub>2</sub>O<sub>3</sub> catalysts. The amount of stored NO<sub>x</sub> at steady state is 0.351 mmol/g<sub>cat</sub> (see Fig. 2A), and a significant decrease is observed upon decreasing the NO/O<sub>2</sub> concentration (see Fig. 2A). The surface FT-IR analysis (Fig. 3D) shows that the main stored species are ionic nitrites ( $\nu_{\text{asym}}(\text{NO}_2)$  and  $\nu_{\text{sym}}(\text{NO}_2)$  modes at 1225 and 1320 cm<sup>-1</sup>, respectively) and linear nitrites ( $\nu(\text{N}=\text{O})$  and  $\nu(\text{N}=\text{O})$  modes at 1077 and 1550 cm<sup>-1</sup>, respectively). Small amounts of bidentate nitrates ( $\nu(\text{N}=\text{O})$  modes at 1610 and 1470 cm<sup>-1</sup>) are also observed.

It is of interest to focus the attention on the shape of the ionic nitrite band at 1215–1230 cm<sup>-1</sup> observed in the different samples. In Fig. 4 the FT-IR spectra recorded during the initial phases of the NO storage (5 min, Fig. 4A) and at steady-state (50 min, Fig. 4B) are compared in the range 1300–1100 cm<sup>-1</sup>. For comparison purposes, the spectra have been normalized on the nitrite band intensity. Over the Ba/Al<sub>2</sub>O<sub>3</sub> catalyst sample (spectrum a), nitrites are stored at BaO sites only, being the alumina support almost completely covered by Ba (as demonstrated by the absence of the stretching band assigned to OH on Al<sub>2</sub>O<sub>3</sub> surface, data here not shown). Nitrites over Pt-Ba/Al<sub>2</sub>O<sub>3</sub> (spectrum c) show features similar to Ba/Al<sub>2</sub>O<sub>3</sub> both at short and prolonged exposures, suggesting that also in this case the storage sites are represented by BaO only. On the other hand, on Pt/Al<sub>2</sub>O<sub>3</sub> system (spectrum b) the storage occurs on Al<sub>2</sub>O<sub>3</sub> sites and the shape of nitrite band at 1230 cm<sup>-1</sup> appears different from that related to nitrites on BaO sites, being slightly asymmetrical and shifted to higher frequencies. Notably, in the case of Pt/Al<sub>2</sub>O<sub>3</sub> + Ba/Al<sub>2</sub>O<sub>3</sub> physical mixture (spectrum d), at the early stage of adsorption the nitrite band closely resembles that observed on Pt/

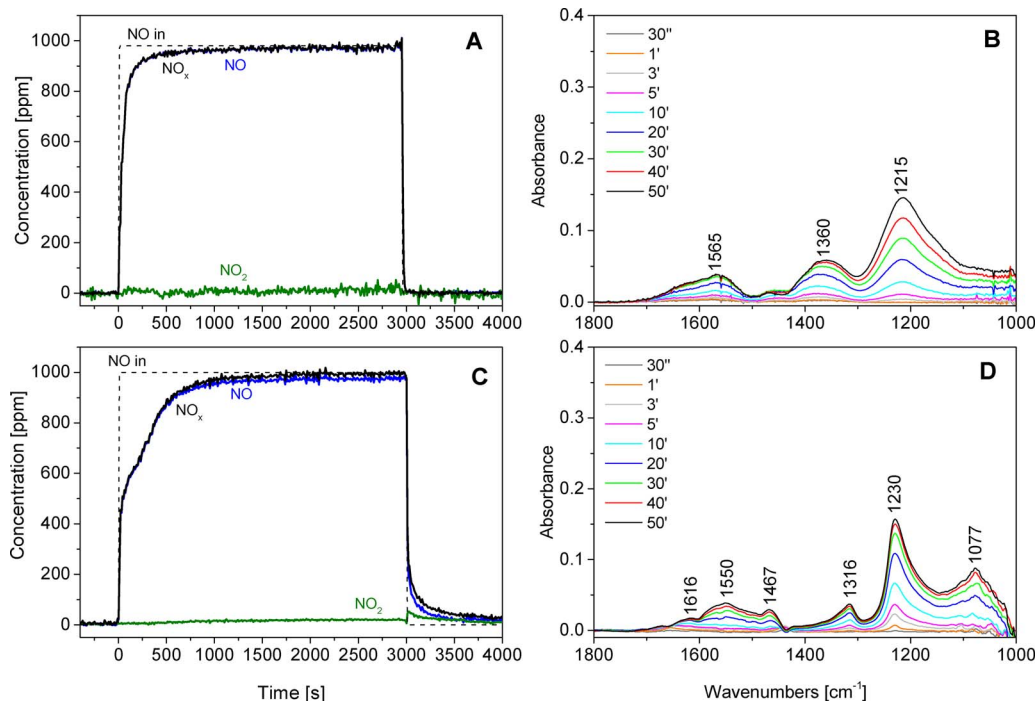


**Fig. 1.** NO/O<sub>2</sub> adsorption at 150 °C over Ba/Al<sub>2</sub>O<sub>3</sub> (A, B) and Pt/Al<sub>2</sub>O<sub>3</sub> (C, D). A, C: gas phase analysis; B, D: surface FT-IR analysis. Storage conditions: 1000 ppm NO + 3% v/v O<sub>2</sub> in He at 150 °C.

Al<sub>2</sub>O<sub>3</sub>, suggesting that the storage occurs initially on the alumina sites. Then, at higher time on stream, another component is identified in the nitrite band with features similar to that observed for Ba/Al<sub>2</sub>O<sub>3</sub> sample, indicating that ionic nitrites are stored on the BaO component as well.

Notably, water (and CO<sub>2</sub> as well) does not significantly affect the pathways for the NO<sub>x</sub> storage, as pointed out by dedicated experiments performed over the same catalyst samples in the presence of water and/or CO<sub>2</sub>. In particular, data obtained over the ternary Pt-Ba/Al<sub>2</sub>O<sub>3</sub> sample, discussed in [24], showed that water has only minor effects on the amounts and nature of the adsorbed NO<sub>x</sub> species. Similar results have been obtained in the presence of CO<sub>2</sub>, although in this case the rate of NO<sub>x</sub> adsorption is slightly decreased. In the presence of water (or CO<sub>2</sub>) the Ba storage sites are present in the form of Ba(OH)<sub>2</sub> (or BaCO<sub>3</sub>) species, but the nitrite route is still operating [22] and Ba nitrite formation from NO/O<sub>2</sub> is occurring upon displacement of water (or CO<sub>2</sub>) from Ba sites. Similar conclusions have been derived for the mechanical mixture as well, based on flow microreactor data (unpublished results).

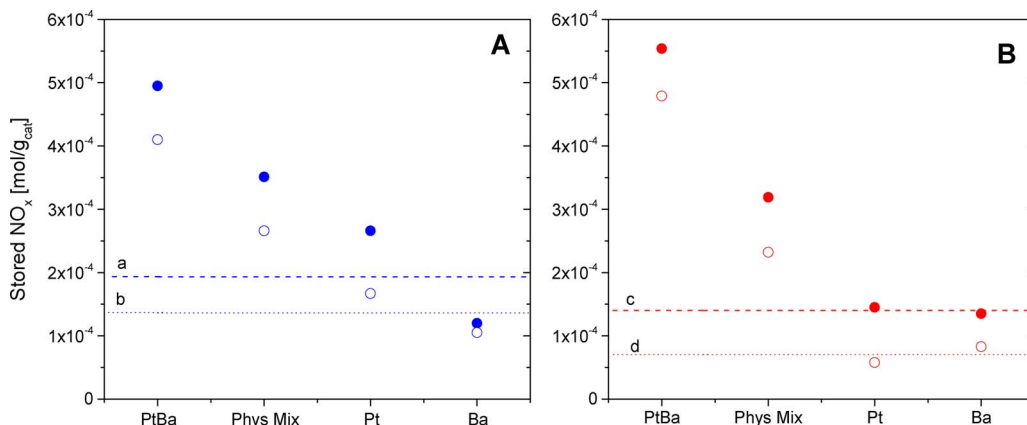
### 3.1.2. Adsorption at 350 °C

Fig. 5 shows the results obtained during the NO<sub>x</sub> storage carried out at 350 °C in the case of the Ba/Al<sub>2</sub>O<sub>3</sub> and Pt/Al<sub>2</sub>O<sub>3</sub> catalysts. On the Ba/Al<sub>2</sub>O<sub>3</sub> sample (Fig. 5A) NO is detected immediately upon admission; the

formation of NO<sub>2</sub> is nihil and the NO<sub>x</sub> adsorption capacity at steady state is limited to 0.135 mmol/g<sub>cat</sub> (Fig. 2B). FT-IR analysis of the surface species (Fig. 5B) shows the formation of ionic nitrites ( $\nu_{\text{asym.}}(\text{NO}_2)$  mode at 1215 cm<sup>-1</sup>) only over BaO sites. However, at variance to what observed at 150 °C, at this temperature negative bands at 1560, 1444 and 1390 cm<sup>-1</sup> appear in the spectra, corresponding to the displacement of carbonates still present on the BaO surface after the conditioning treatment. These negative bands increase in intensity on increasing the amounts of stored nitrites.

On Pt/Al<sub>2</sub>O<sub>3</sub> (Fig. 5C) the dead time for NO<sub>x</sub> breakthrough is nihil, but at steady-state 0.145 mmol/g<sub>cat</sub> of NO<sub>x</sub> have been stored, see Fig. 2B. Besides, the NO/NO<sub>2</sub> oxidation is effective, being the amount of NO<sub>2</sub> formed at steady state near 440 ppm. As shown by FT-IR analysis (Fig. 5D), NO<sub>x</sub> are initially stored over alumina in the form of nitrites ( $\nu_{\text{asym.}}(\text{NO}_2)$  mode at 1235 cm<sup>-1</sup>); these species then rapidly evolve to bidentate nitrates ( $\nu(\text{N}=\text{O})$  modes at 1610, 1580 and 1565 cm<sup>-1</sup>,  $\nu_{\text{asym.}}(\text{NO}_2)$  modes at 1297 and 1250 cm<sup>-1</sup> and  $\nu_{\text{sym.}}(\text{NO}_2)$  mode at 1037 cm<sup>-1</sup>). Indeed, the considerable amounts of NO<sub>2</sub> detected in the gas phase can be adsorbed as nitrates and oxidize nitrites into nitrates as well [8].

Fig. 6A, C shows the results of the gas phase analysis obtained during the NO<sub>x</sub> storage at 350 °C over Pt-Ba/Al<sub>2</sub>O<sub>3</sub> and Pt/Al<sub>2</sub>O<sub>3</sub> + Ba/



**Fig. 2.** NO<sub>x</sub> stored amount (expressed in mol/g<sub>cat</sub>) estimated for Ba/Al<sub>2</sub>O<sub>3</sub>, Pt/Al<sub>2</sub>O<sub>3</sub>, Pt-Ba/Al<sub>2</sub>O<sub>3</sub> and Pt/Al<sub>2</sub>O<sub>3</sub> + Ba/Al<sub>2</sub>O<sub>3</sub> physical mixture systems. A) 150 °C and B) 350 °C. Full symbols correspond to the amounts stored at steady state, empty symbols to that stored after NO/O<sub>2</sub> shutoff. Horizontal lines: theoretical NO<sub>x</sub> stored amount estimated from the sum of Pt/Al<sub>2</sub>O<sub>3</sub> and Ba/Al<sub>2</sub>O<sub>3</sub> samples. Dashed lines (a, c): NO<sub>x</sub> stored at steady state; dotted lines (b, d): NO<sub>x</sub> stored after NO/O<sub>2</sub> shutoff.

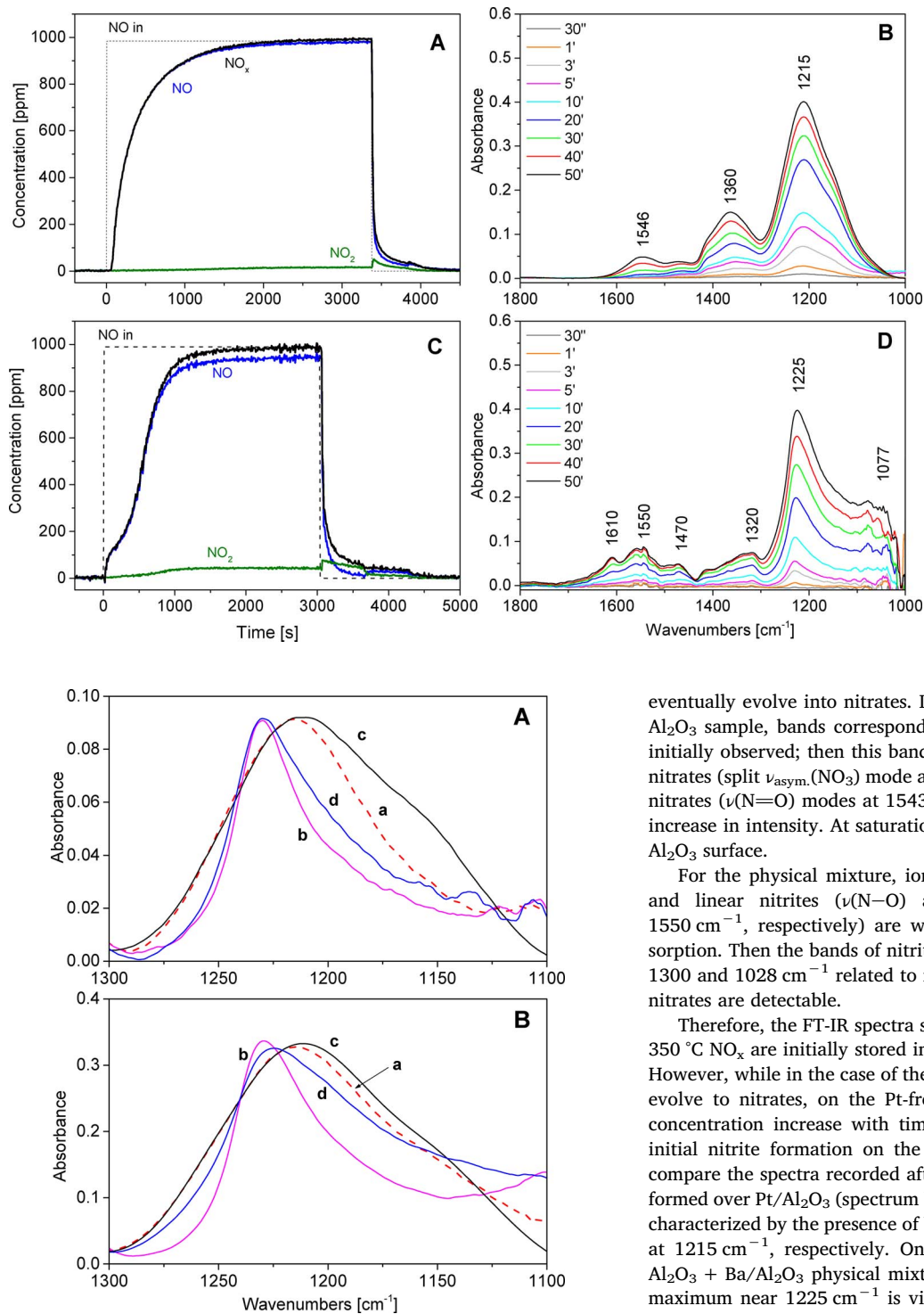


**Fig. 3.** NO/O<sub>2</sub> adsorption at 150 °C over Pt-Ba/Al<sub>2</sub>O<sub>3</sub> catalyst (A, B) and Pt/Al<sub>2</sub>O<sub>3</sub> + Ba/Al<sub>2</sub>O<sub>3</sub> physical mixture (C, D). A, C: gas phase analysis; B, D: surface FT-IR analysis. Storage conditions: 1000 ppm NO + 3% v/v O<sub>2</sub> in He at 150 °C.

eventually evolve into nitrates. In particular, in the case of the Pt-Ba/Al<sub>2</sub>O<sub>3</sub> sample, bands corresponding to ionic nitrites (1215 cm<sup>-1</sup>) are initially observed; then this band decreases and bands related to ionic nitrates (split  $\nu_{\text{asym}}(\text{NO}_3)$  mode at 1415 and 1320 cm<sup>-1</sup>) and bidentate nitrates ( $\nu(\text{N}=\text{O})$  modes at 1543 and  $\nu_{\text{sym}}(\text{NO}_2)$  mode at 1037 cm<sup>-1</sup>) increase in intensity. At saturation, only nitrates are present on Pt-Ba/Al<sub>2</sub>O<sub>3</sub> surface.

For the physical mixture, ionic ( $\nu_{\text{asym}}(\text{NO}_2)$  mode at 1225 cm<sup>-1</sup>) and linear nitrites ( $\nu(\text{N}=\text{O})$  and  $\nu(\text{N}=\text{O})$  modes at 1077 and 1550 cm<sup>-1</sup>, respectively) are well visible at the initial stage of adsorption. Then the bands of nitrites decrease and bands at 1565, 1408, 1300 and 1028 cm<sup>-1</sup> related to nitrates increase. At steady-state, only nitrates are detectable.

Therefore, the FT-IR spectra showed in Fig. 5 and 6 indicate that at 350 °C NO<sub>x</sub> are initially stored in the form of nitrites over all samples. However, while in the case of the Pt-containing systems nitrites readily evolve to nitrates, on the Pt-free sample (i.e. Ba/Al<sub>2</sub>O<sub>3</sub>) the nitrite concentration increase with time on stream. Notably, regarding the initial nitrite formation on the various samples, it is of interest to compare the spectra recorded after 1 min of storage (Fig. 7A). Nitrites formed over Pt/Al<sub>2</sub>O<sub>3</sub> (spectrum b) and over Ba/Al<sub>2</sub>O<sub>3</sub> (spectrum a) are characterized by the presence of bands with maxima at 1235 cm<sup>-1</sup> and at 1215 cm<sup>-1</sup>, respectively. On the other hand, in the case of Pt/Al<sub>2</sub>O<sub>3</sub> + Ba/Al<sub>2</sub>O<sub>3</sub> physical mixture (spectrum d), a broad band with maximum near 1225 cm<sup>-1</sup> is visible, likely resulting from the superposition of the nitrite bands observed at 1235 cm<sup>-1</sup> on Pt/Al<sub>2</sub>O<sub>3</sub> (spectrum b) and at 1215 cm<sup>-1</sup> on Ba/Al<sub>2</sub>O<sub>3</sub> (spectrum a). This indicates that in the physical mixture the NO<sub>x</sub> storage is simultaneously occurring on both the Al and Ba sites of the Pt/Al<sub>2</sub>O<sub>3</sub> and Ba/Al<sub>2</sub>O<sub>3</sub> particles, respectively. The subsequent evolution of nitrites into nitrates (over the Pt-containing samples) may be ascribed to the oxidation by NO<sub>2</sub> that in fact is detected in significant amounts in the gas phase. In the case of the physical mixture, oxidation involves nitrites stored on both Al<sub>2</sub>O<sub>3</sub> and Ba as pointed out by the presence of nitrates on both these sites. In fact, the bidentate nitrates with  $\nu(\text{N}=\text{O})$  band at 1565 cm<sup>-1</sup> correspond to nitrate species on Al<sub>2</sub>O<sub>3</sub> sites of the Pt/Al<sub>2</sub>O<sub>3</sub> particle in the mixture, whereas bands in the region 1500–1300 cm<sup>-1</sup> (not present in the case of the Pt/Al<sub>2</sub>O<sub>3</sub> sample) are related to ionic

**Fig. 4.** Surface FT-IR analysis (1100–1300 cm<sup>-1</sup> range) during NO/O<sub>2</sub> adsorption at 150 °C over Ba/Al<sub>2</sub>O<sub>3</sub> (curve a), Pt/Al<sub>2</sub>O<sub>3</sub> (curve b), Pt-Ba/Al<sub>2</sub>O<sub>3</sub> (curve c) and Pt/Al<sub>2</sub>O<sub>3</sub> + Ba/Al<sub>2</sub>O<sub>3</sub> physical mixture (curve d) systems after 5 min of exposure (A) and 50 min of exposure (B).

Al<sub>2</sub>O<sub>3</sub> physical mixture, respectively. The quantitative analysis (Fig. 2B) shows that significant amounts of NO<sub>x</sub> are stored at steady state (0.554 mmol/g<sub>cat</sub> and 0.319 mmol/g<sub>cat</sub>, respectively for Pt-Ba/Al<sub>2</sub>O<sub>3</sub> and Pt/Al<sub>2</sub>O<sub>3</sub> + Ba/Al<sub>2</sub>O<sub>3</sub> physical mixture). A dead time for NO<sub>x</sub> breakthrough is observed in the case of Pt-Ba/Al<sub>2</sub>O<sub>3</sub> near 260 s while it is nihil in the case of the physical mixture. FT-IR analysis (Fig. 6B and D for Pt-Ba/Al<sub>2</sub>O<sub>3</sub> and the physical mixture, respectively), shows that for both samples NO<sub>x</sub> are stored initially in the form of nitrites that

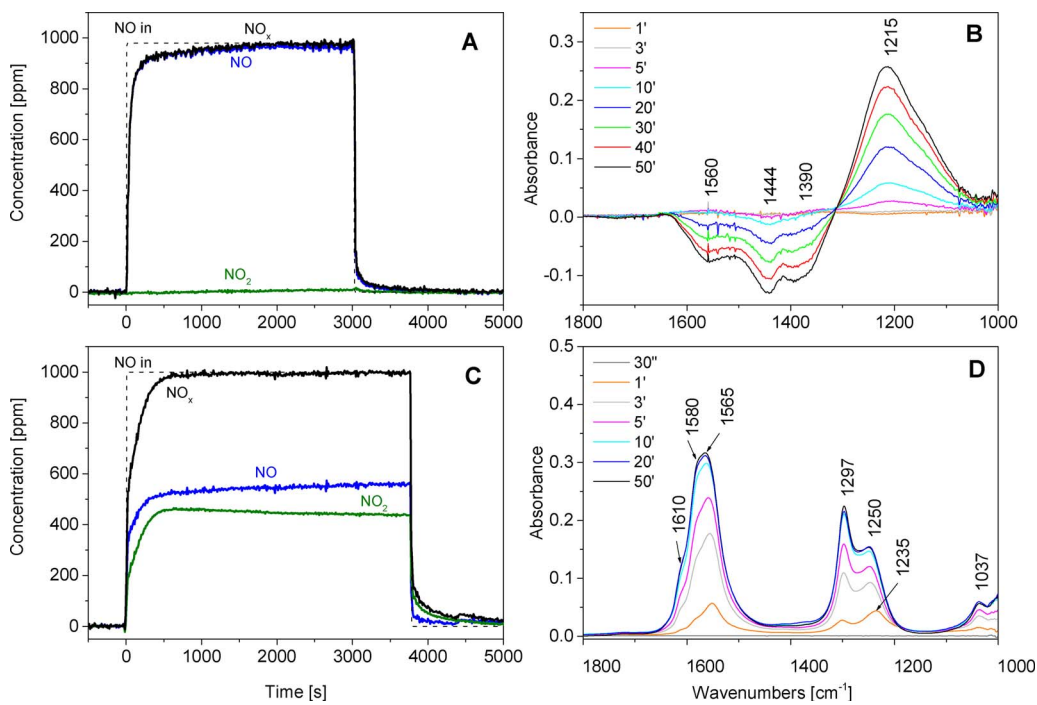


**Fig. 5.** NO/O<sub>2</sub> adsorption at 350 °C over Ba/Al<sub>2</sub>O<sub>3</sub> (A, B) and Pt/Al<sub>2</sub>O<sub>3</sub> (C, D). A, C: gas phase analysis; B, D: surface FT-IR analysis. Storage conditions: 1000 ppm NO + 3% v/v O<sub>2</sub> in He at 350 °C.

nitrates on BaO sites of Ba/Al<sub>2</sub>O<sub>3</sub>. These ionic species are the same observed in the case of the Pt-Ba/Al<sub>2</sub>O<sub>3</sub> catalyst.

At 350 °C the amount of NO<sub>x</sub> stored at steady-state (mmol/g<sub>cat</sub>) increases in the order: Pt-Ba/Al<sub>2</sub>O<sub>3</sub> > physical mixture > Pt/Al<sub>2</sub>O<sub>3</sub> ≈ Ba/Al<sub>2</sub>O<sub>3</sub> (Fig. 2B), and therefore the ternary catalyst outperforms the Pt/Al<sub>2</sub>O<sub>3</sub> + Ba/Al<sub>2</sub>O<sub>3</sub> physical mixture. Note that any correlation holds between the NO oxidation capability to NO<sub>2</sub> and the NO<sub>x</sub> storage properties. Indeed, the physical mixture provides a higher NO<sub>2</sub>/NO molar ratio than the Pt-Ba/Al<sub>2</sub>O<sub>3</sub> system, but this sample, where Pt and Ba are dispersed over the same particle support, provides the best storage capacity in spite of the lower NO oxidation properties (i.e. lower NO<sub>2</sub>/NO molar ratio).

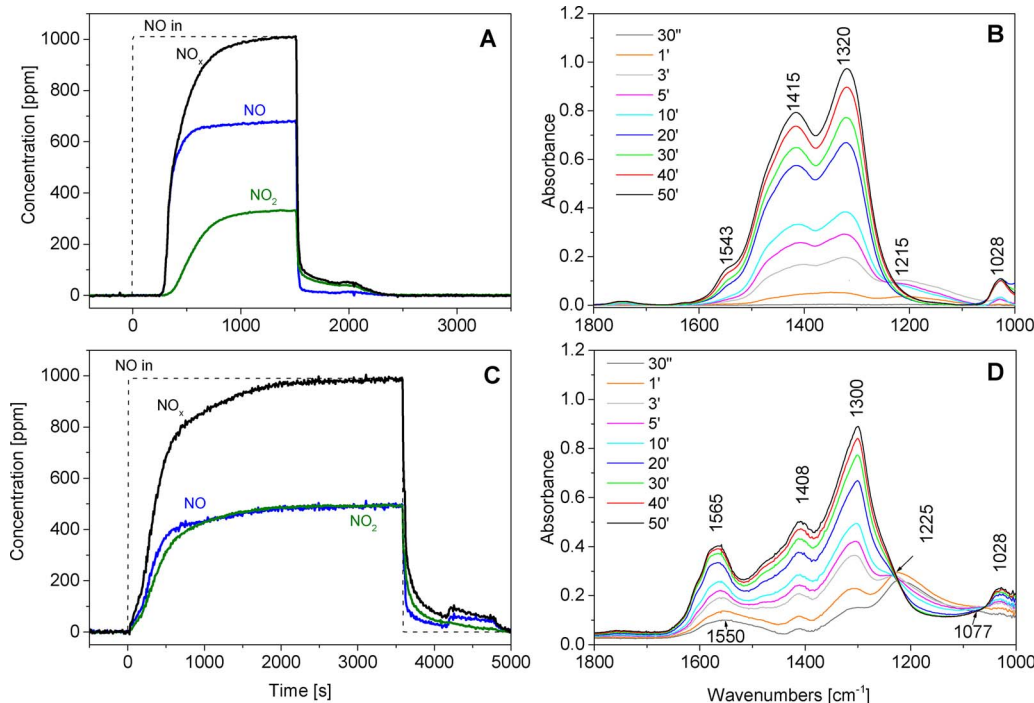


**Fig. 6.** NO/O<sub>2</sub> adsorption at 350 °C over Pt-Ba/Al<sub>2</sub>O<sub>3</sub> catalyst (A, B) and Pt/Al<sub>2</sub>O<sub>3</sub> + Ba/Al<sub>2</sub>O<sub>3</sub> physical mixture (C, D). A, C: gas phase analysis; B, D: surface FT-IR analysis. Storage conditions: 1000 ppm NO + 3% v/v O<sub>2</sub> in He at 350 °C.

As reported in [24] (and references therein) water (and CO<sub>2</sub>) does not significantly affect the NO<sub>x</sub> storage at high temperatures, as expected. However, CO<sub>2</sub> inhibits the transient nitrite formation at high temperature, due to the different thermal stability of nitrites and carbonates [24].

### 3.2. Mechanistic insights of the NO/O<sub>2</sub> adsorption

A sketch of the pathways involved in the NO/O<sub>2</sub> adsorption at 150 °C are shown in Fig. 8. At these temperatures, nitrites are formed upon contacting the various samples with the NO/O<sub>2</sub> mixture, if one neglects very tiny amounts of nitrates detected in few cases. In the case

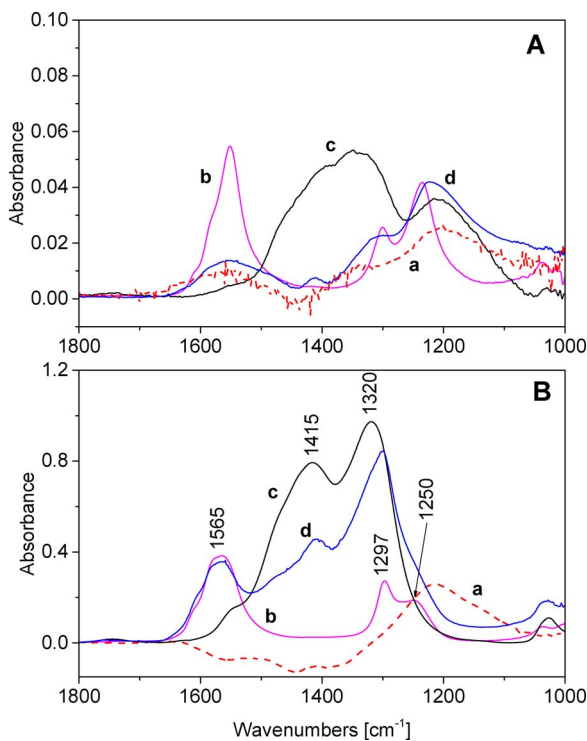


Fig. 7. Surface FT-IR analysis (1000–1800 cm<sup>-1</sup> range) during NO/O<sub>2</sub> adsorption at 350 °C over Ba/Al<sub>2</sub>O<sub>3</sub> (curve a), Pt/Al<sub>2</sub>O<sub>3</sub> (curve b), Pt-Ba/Al<sub>2</sub>O<sub>3</sub> (curve c) and Pt/Al<sub>2</sub>O<sub>3</sub> + Ba/Al<sub>2</sub>O<sub>3</sub> physical mixture (curve d) systems after 1 min of exposure (A) and 50 min of exposure (B).

of the Ba/Al<sub>2</sub>O<sub>3</sub> catalyst, the amount of stored nitrites is low but yet appreciable (see Fig. 2A). It is likely that these species are formed (Fig. 8A) by interaction of NO/O<sub>2</sub> with O<sub>(s)</sub><sup>2-</sup> surface oxygen anion (e.g. lattice oxygen of Ba sites), according to the overall stoichiometry of reaction (1):



The rate of adsorption at this temperature is rather low and therefore the nitrite concentration slowly increases with time on stream (see Fig. 1B).

A similar pathway is likely to operate in the case of the Pt/Al<sub>2</sub>O<sub>3</sub> catalyst as well (Fig. 8B), as pointed out by FT-IR spectra showing the progressive formation of nitrites species (Fig. 1 D). However in this case, nitrites are stored over the alumina support, and the nature of the

formed nitrites is different from that observed over Ba sites due to the different basicity of the adsorption sites. It is worth to note that in the case of Pt/Al<sub>2</sub>O<sub>3</sub> catalyst, the presence of oxygen in the feed is essential to form adsorbed species. Indeed, previous data showed that in the absence of oxygen NO is adsorbed in negligible amounts on the Pt/Al<sub>2</sub>O<sub>3</sub> sample [25]. Over Pt/Al<sub>2</sub>O<sub>3</sub> the adsorption is faster than on Ba/Al<sub>2</sub>O<sub>3</sub> (as pointed out by the slower rise of the outlet NO<sub>x</sub> concentration, see Fig. 1C) and higher amount of NO<sub>x</sub> are stored (Fig. 2A). This is related to the presence of Pt sites, which are involved in the activation of O<sub>2</sub>/NO molecules providing the required oxygen species for the storage in the form of nitrites. Notably, significant amounts of nitrites can be stored in spite of the very poor NO to NO<sub>2</sub> oxidation. Accordingly, the stoichiometry of reaction (1) represents an effective pathway for the storage of NO<sub>x</sub>, pointing out that the NO oxidation to NO<sub>2</sub> is not required to store nitrites on the surface. However, NO<sub>2</sub>, when formed, may also participate in the storage of nitrites, as will be discussed below.

The nitrites species stored over Pt/Al<sub>2</sub>O<sub>3</sub> sample are less stable than those adsorbed over Ba/Al<sub>2</sub>O<sub>3</sub>. In fact, a significant tail is observed upon the NO/O<sub>2</sub> shut off in the case of the Pt/Al<sub>2</sub>O<sub>3</sub>, leading to a significant decrease of the amounts of NO<sub>x</sub> stored (see Fig. 2A).

The Pt/Al<sub>2</sub>O<sub>3</sub> + Ba/Al<sub>2</sub>O<sub>3</sub> physical mixture is able to store more NO<sub>x</sub> than those expected from the sum of the individual Pt/Al<sub>2</sub>O<sub>3</sub> and Ba/Al<sub>2</sub>O<sub>3</sub> samples (represented by the horizontal line in Fig. 2). This indicates a synergistic effect between the binary Pt/Al<sub>2</sub>O<sub>3</sub> and Ba/Al<sub>2</sub>O<sub>3</sub> catalysts. As suggested in Fig. 8C, this synergistic effect is explained through the formation of NO<sub>2</sub> (over Pt/Al<sub>2</sub>O<sub>3</sub>) followed by its migration in the gas phase and participation in the storage of nitrites over the Ba/Al<sub>2</sub>O<sub>3</sub> catalyst particles.

To check the impact of the presence of small amounts of NO<sub>2</sub> in the storage of nitrites over Ba, experiments have been performed over the single Ba/Al<sub>2</sub>O<sub>3</sub> catalyst where a mixture of NO + NO<sub>2</sub> (1000 ppm + 60 ppm) in the presence of O<sub>2</sub> (3% v/v) in He has been used during the storage phase. Both the gas phase and FT-IR analysis (data here not reported) showed a significant increase in the amounts of nitrites stored onto the Ba component. These results parallel data from the group of Iglesia [26] showing that over BaO/Al<sub>2</sub>O<sub>3</sub> nitrites are formed upon vicinal co-adsorption of NO and NO<sub>2</sub> molecules, possibly via the following disproportion reaction:



Therefore, it is likely that small amounts of NO<sub>2</sub> formed upon NO oxidation over the Pt component enhance, via migration in the gas-phase, the NO<sub>x</sub> storage in the form of nitrites over Ba sites far away from Pt (Fig. 8C). This is also in line with the observation (see Fig. 4)

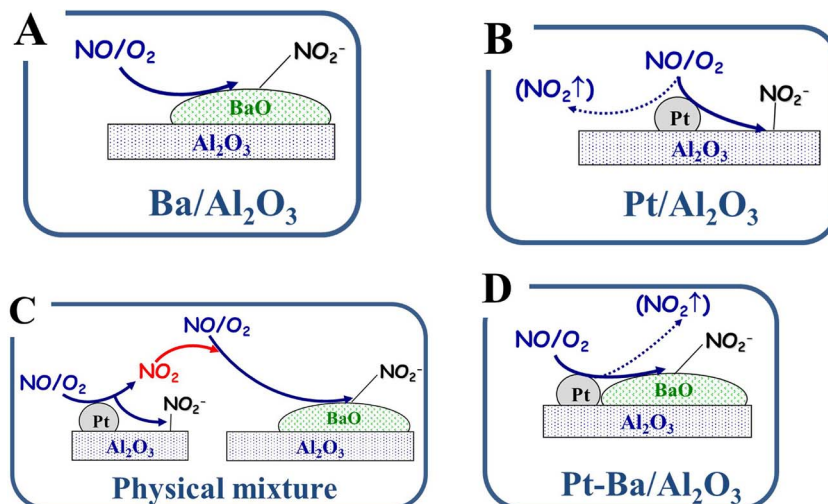


Fig. 8. Sketch of NO<sub>x</sub> storage mechanism at 150 °C over A) Ba/Al<sub>2</sub>O<sub>3</sub>; B) Pt/Al<sub>2</sub>O<sub>3</sub>; C) Pt/Al<sub>2</sub>O<sub>3</sub> + Ba/Al<sub>2</sub>O<sub>3</sub> physical mixture; D) Pt-Ba/Al<sub>2</sub>O<sub>3</sub> systems.

that in the physical mixture nitrite formation occurs initially on the alumina sites of  $\text{Pt}/\text{Al}_2\text{O}_3$ , and then on the Ba sites of the  $\text{Ba}/\text{Al}_2\text{O}_3$  sample.

Over the  $\text{Pt-Ba}/\text{Al}_2\text{O}_3$  catalyst (Fig. 8D) nitrites are formed onto the Ba sites, as already discussed, being the alumina support completely covered by Ba. Accordingly, the  $\text{NO}_x$  storage occurs according to the stoichiometry of reaction (1) where  $\text{O}_{(s)}^{2-}$  are surface oxygen anion from Ba species. Notably, in this case the amount of  $\text{NO}_x$  stored at steady state is much higher than the individual  $\text{Pt}/\text{Al}_2\text{O}_3$  and  $\text{Ba}/\text{Al}_2\text{O}_3$  samples and of the physical mixture as well (Fig. 2A). Also, the rate of  $\text{NO}_x$  adsorption (due to nitrite formation) is high as pointed out by the presence of a dead time for  $\text{NO}_x$  breakthrough (indicating complete  $\text{NO}_x$  storage) and by the subsequent slow increase in the  $\text{NO}_x$  outlet concentration (Fig. 3A). This clearly indicates that the close proximity between Pt and Ba sites greatly enhances the  $\text{NO}_x$  storage through a cooperative between the Ba storage sites and the Pt oxidation sites that activate oxygen (and possibly NO as well) [27,28]. Oxygen activated over Pt then spills over to the storage sites thus making possible the NO oxidation/adsorption in the form of nitrites. This picture is consistent with our previous findings [22] and with results of Chaugule et al. [29] who reported that Ba sites vicinal to Pt are responsible for the so-called “fast”  $\text{NO}_x$  storage, leading to the presence of a dead time for  $\text{NO}_x$  breakthrough. It is also consistent with the effect of ageing where a deterioration of the storage properties is observed due to the decrease of the Pt/Ba interface upon Pt sintering [16].

The pathways involved in the  $\text{NO}_x$  adsorption at high temperature (350 °C) are shown in the scheme of Fig. 9. Also at this temperature over all the investigated systems nitrites are initially formed, as shown by FT-IR spectra previously discussed. Nitrite formation occurs according to the lines previously discussed, i.e. according to the stoichiometry of reaction (1) where  $\text{O}_{(s)}^{2-}$  surface anions correspond to

lattice oxygen of  $\text{Al}_2\text{O}_3$  and/or Ba sites (see Fig. 9B and A, respectively). However, over the Pt-containing samples, at 350 °C (see Figs. 5 and 6) significant amounts of  $\text{NO}_2$  are also formed, and nitrates are also apparent along with nitrites at the early stages of adsorption. Notably, nitrite species rapidly disappear being transformed into nitrate species so that at the end of the storage only nitrates are present on the catalyst surface. At variance, over the Pt-free  $\text{Ba}/\text{Al}_2\text{O}_3$  sample, formation of nitrites only is observed.

$\text{NO}_2$  formation is due to the oxidation of NO by  $\text{O}_2$  over Pt, a fast reaction at high temperatures:



$\text{NO}_2$  may participate with NO in nitrite formation, along the lines previously discussed, and in the formation of nitrites/nitrates adspecies following the stoichiometry of the following disproportion reaction (4):



Reaction (4), along with reaction (1), may explain the initial formation of nitrites and nitrates at the early stages of adsorption, as sketched in Fig. 9B–D. Over the Pt-containing systems, nitrites are eventually oxidized to nitrates (Fig. 9B–D) by  $\text{O}_2$  according to the stoichiometry of reaction (5):

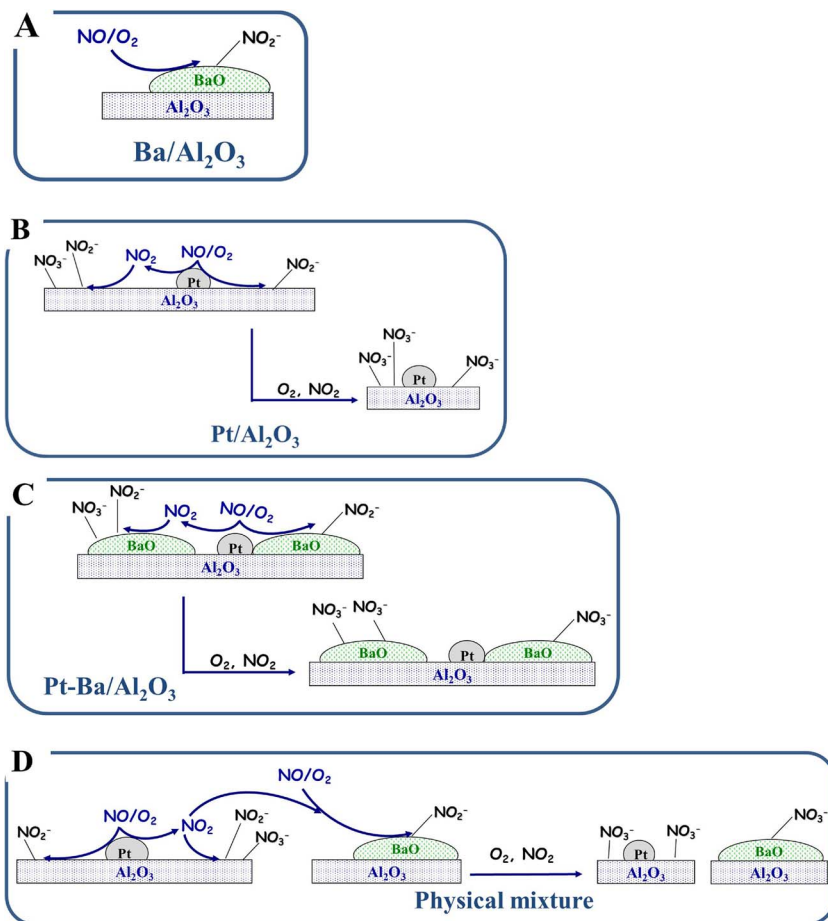


or by  $\text{NO}_2$  according to the stoichiometry of reaction (6):



Note that nitrite oxidation may take place by  $\text{N}_2\text{O}_4$  that is produced by non-activated bimolecular collisions of  $\text{NO}_2$  molecules in the gas phase, according to reactions (7)–(8) [26]:

**Fig. 9.** Sketch of  $\text{NO}_x$  storage mechanism at 350 °C over A)  $\text{Ba}/\text{Al}_2\text{O}_3$ ; B)  $\text{Pt}/\text{Al}_2\text{O}_3$ ; C)  $\text{Pt-Ba}/\text{Al}_2\text{O}_3$ ; D)  $\text{Pt}/\text{Al}_2\text{O}_3 + \text{Ba}/\text{Al}_2\text{O}_3$  physical mixture systems.



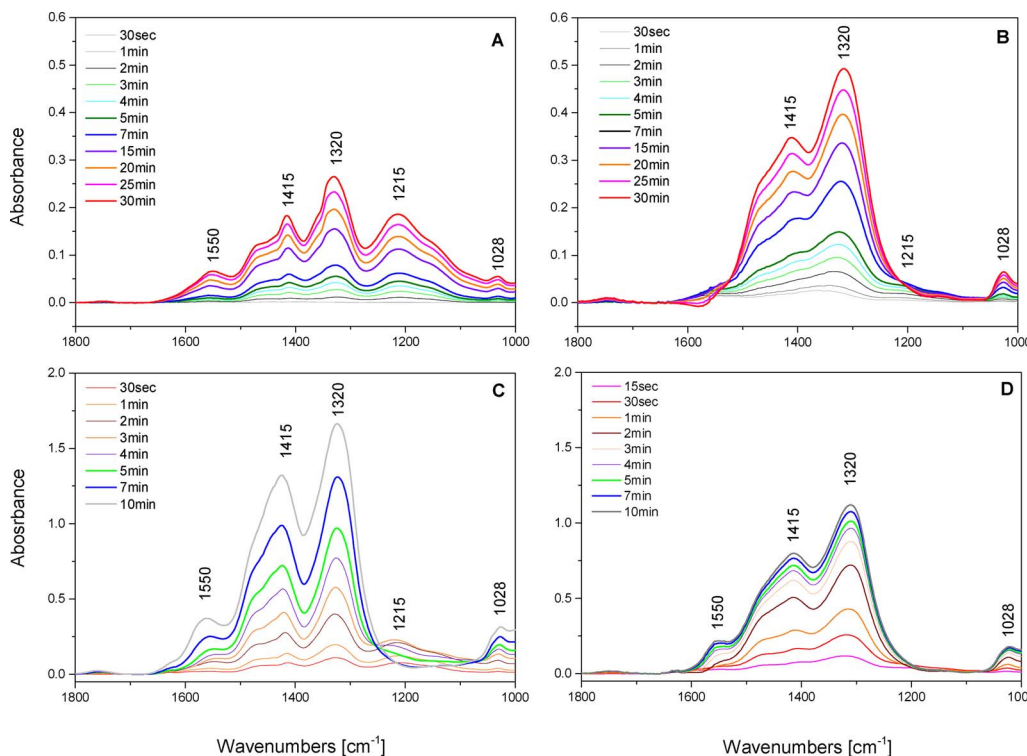
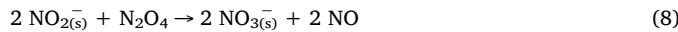
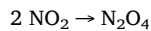


**Fig. 10.** Surface FT-IR analysis during  $\text{NO}_2$  adsorption at 150 °C (A, C) and 350 °C (B, D) over Pt-Ba/Al<sub>2</sub>O<sub>3</sub>; A, B (70 ppm  $\text{NO}_2$ ); C, D (1000 ppm  $\text{NO}_2$ ).



When the  $\text{NO}_2$  concentration is small (i.e. at 150 °C where reaction (3) occurs to a much lower extent), the formation of  $\text{N}_2\text{O}_4$  is less likely and nitrites are not oxidized into nitrates. On the other hand,  $\text{NO}_2$  participates in nitrite formation according to the lines previously discussed.

To further investigate the role of  $\text{NO}_2$  in the nitrite/nitrate formation and in their transformation into nitrates (i.e. reactions (4) and (6)), additional FT-IR experiments have been carried out over the Pt-Ba/Al<sub>2</sub>O<sub>3</sub> catalyst where the  $\text{NO}_2$  adsorption in He has been carried out at different concentrations (70 ppm and 1000 ppm) at both 150 °C and 350 °C, and results are shown in Fig. 10. At 150 °C (Fig. 10A and C) the formation of nitrites (band at 1215  $\text{cm}^{-1}$ ) and of nitrates (bands at 1550, 1415, 1320 and 1028  $\text{cm}^{-1}$ ) is observed both at low (70 ppm) and high (1000 ppm)  $\text{NO}_2$  concentration. However, differences are observed in their evolution with time. In fact, at low  $\text{NO}_2$  concentration (Fig. 10A) nitrites and nitrates are formed simultaneously according to reaction (4), and their concentration simultaneously increases on increasing the contact time. At variance, at high  $\text{NO}_2$  concentration (1000 ppm, Fig. 10C), nitrites and nitrates are formed simultaneously at low contact time; after 4 min the nitrate bands continue to increase whereas the nitrite band at 1215  $\text{cm}^{-1}$  starts to decrease, being nitrites oxidized into nitrates by  $\text{NO}_2$  or  $\text{N}_2\text{O}_4$  (reactions (6) and (8), respectively).

At high temperature (350 °C, Fig. 10B and D) extensive nitrate formation is observed while very small amounts of nitrites are observed only at the very early stage of adsorption, and for low  $\text{NO}_2$  concentration only (Fig. 10B). In fact, at such high temperature the rate of reactions (4) and (6) is very high so that nitrites, which are initially formed along with nitrates, are readily converted into nitrates and are hardly (or even not visible) in the spectra.

These results are of note since they clearly point out the role of  $\text{NO}_2$  in nitrite/nitrate formation and in the subsequent transformation of nitrites into nitrates.

Worth to note, the discussed pathways for  $\text{NO}_x$  adsorption holds in

the presence of water and  $\text{CO}_2$  as well. In the presence of these species the Ba storage sites are present as Ba hydroxide and carbonates, respectively. Formation of nitrites and nitrates displaces water and  $\text{CO}_2$  from surface hydroxide and carbonates [30], respectively, but the  $\text{NO}_x$  storage is not significantly affected [22]. However small changes in the spectroscopic features of the adsorbed nitrates have been reported due to the presence of water, i.e. from bidentate to ionic species [31,32].

### 3.3. Thermal decomposition of the stored $\text{NO}_x$ species

The thermal decomposition of the species stored at both 150 °C and 350 °C has been investigated by means of TPD experiments. The results obtained after storage of  $\text{NO}_x$  at 150 °C (nitrites) onto Ba/Al<sub>2</sub>O<sub>3</sub>, Pt/Al<sub>2</sub>O<sub>3</sub>, Pt/Al<sub>2</sub>O<sub>3</sub> + Ba/Al<sub>2</sub>O<sub>3</sub> and Pt-Ba/Al<sub>2</sub>O<sub>3</sub> are shown in Fig. 11A–D, respectively. The data obtained in the case of the Pt-Ba/Al<sub>2</sub>O<sub>3</sub> catalyst have already been published elsewhere [21] but are here reported for comparison purposes.

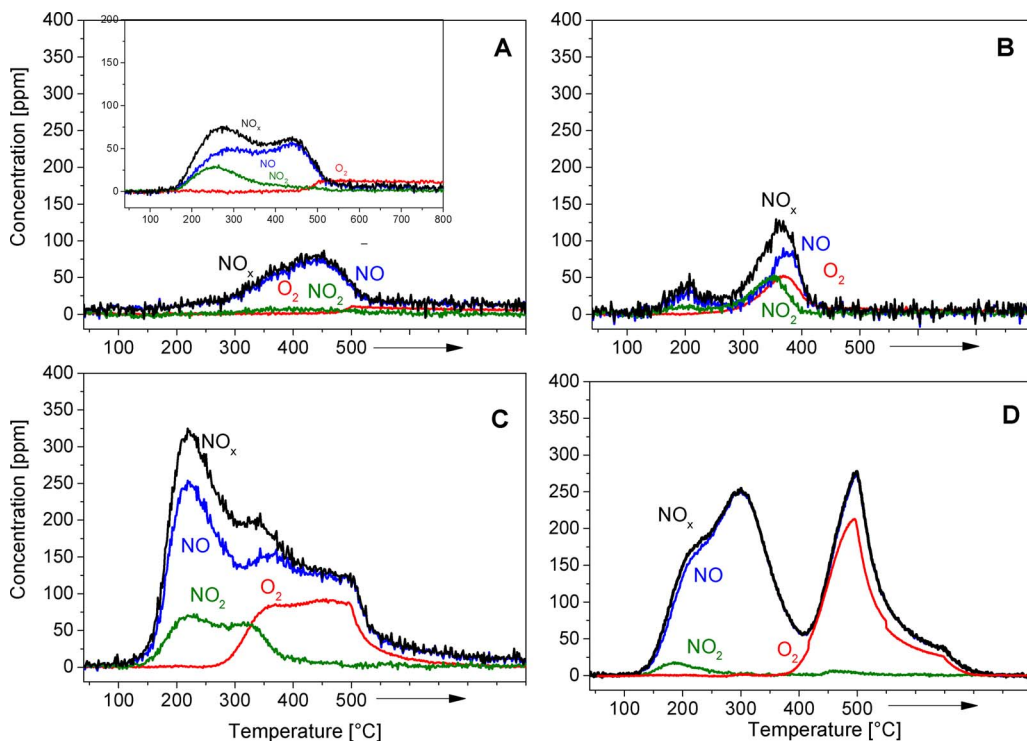
In the case of the Ba/Al<sub>2</sub>O<sub>3</sub> catalyst, the onset temperature for nitrite decomposition is observed above 150 °C (Fig. 11A). NO is detected (peak maximum at 430 °C) in the desorption products along with minor amounts of  $\text{NO}_2$ . A small oxygen evolution is also observed, starting from 470 °C and during the hold at 500 °C at the end of the heating ramp. Fig. 12A, showing the FT-IR spectra recorded during the TPD experiment, indicates that the nitrite bands slowly decrease in intensity with temperature. A fraction of the nitrites stored on the catalyst surface is still present at the end of the heating ramp at 500 °C.

The decomposition of Ba nitrites should result in the evolution of gaseous species having a N/O ratio equal to 0.6. A lack of O atoms in the decomposition products is observed in this case, possibly suggesting the formation of Ba peroxide species, reaction (9) [25]:



The  $\text{O}_2$  desorption observed at high temperatures (above 500 °C) could be associated to the peroxide decomposition formed during the nitrite thermal desorption.

The results obtained during the TPD experiment carried out over the same Ba/Al<sub>2</sub>O<sub>3</sub> catalyst after  $\text{NO}/\text{NO}_2$  adsorption (100/6 molar ratio) at

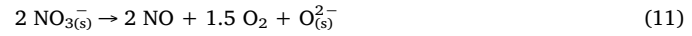


150 °C are shown in the inset of Fig. 11A for comparison purposes. As previously discussed, the adsorption of NO/NO<sub>2</sub> mixtures (with high NO/NO<sub>2</sub> ratio) leads to a significant increase of the amounts of stored nitrites. From the insert in Fig. 11A, it clearly appears that the increase in the nitrite surface concentration leads to a significant increase in the evolution of NO + NO<sub>2</sub> at low temperatures.

The results of the TPD run carried out over the Pt/Al<sub>2</sub>O<sub>3</sub> sample after NO<sub>x</sub> adsorption at 150 °C are shown in Fig. 11B. A small NO peak is observed with onset at 130 °C and maximum at 200 °C along with lower amounts of NO<sub>2</sub>; a second NO peak with much higher intensity and accompanied by O<sub>2</sub> and NO<sub>2</sub> evolution is detected starting from 300 °C and with maximum at 370 °C. FT-IR spectra (Fig. 12B) reveal the initial decrease of the nitrite band at 1550 cm<sup>-1</sup>; then, starting from 180 °C, the band at 1565 cm<sup>-1</sup> (nitrate species) starts to increase, up to 340 °C. Above this temperature, the bands of nitrates starts to decrease as well, and only minor amounts of nitrates are left on the catalyst surface after heating up to 500 °C. The data indicate that nitrites stored over Pt/Al<sub>2</sub>O<sub>3</sub> are partially decomposed to NO<sub>x</sub>/O<sub>2</sub> starting from 150 °C. However, nitrites are also involved in a disproportion reaction leading to nitrates and NO that is released in the gas phase, reaction (10):



At high temperatures, above 300 °C, also nitrates decompose according to reaction (11):



leading to the evolution of NO and oxygen. Note that the sum of reactions (10) and (11) gives the global reaction (12) that describes the decomposition of nitrites to NO and O<sub>2</sub>:



Notably, in the case of nitrites decomposition the expected N/O atomic ratio in the evolved products is 0.6, as can be estimated from the stoichiometry of reaction (12). This value is in fact approached considering the whole amounts of the products (NO, NO<sub>2</sub> and O<sub>2</sub>) evolved during the TPD run. However, the instantaneous N/O atomic ratio estimated during the TPD experiment changes with temperature being near 0.8 in the low temperature region (where the evolution of mainly NO is observed) and approaching 0.4 in the high temperature region. Notably, this N/O value is consistent with the decomposition of nitrates. Therefore, the presence of Pt affects the decomposition of the stored species by catalyzing the nitrite disproportion reaction (10) to

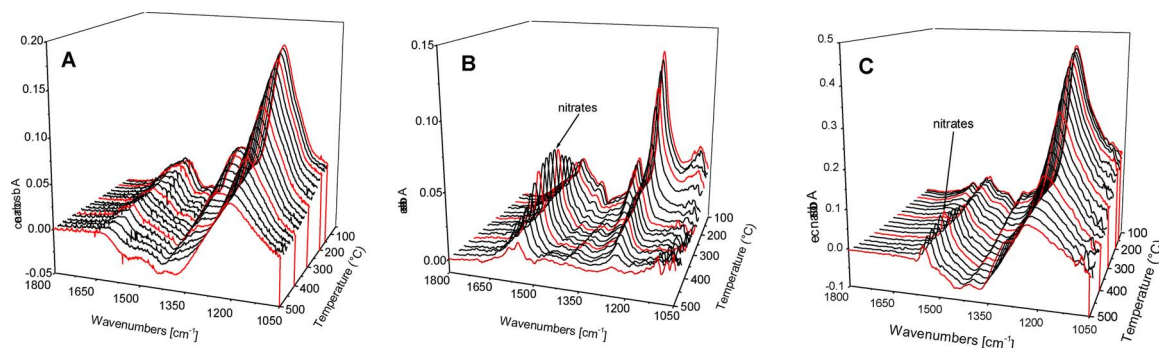
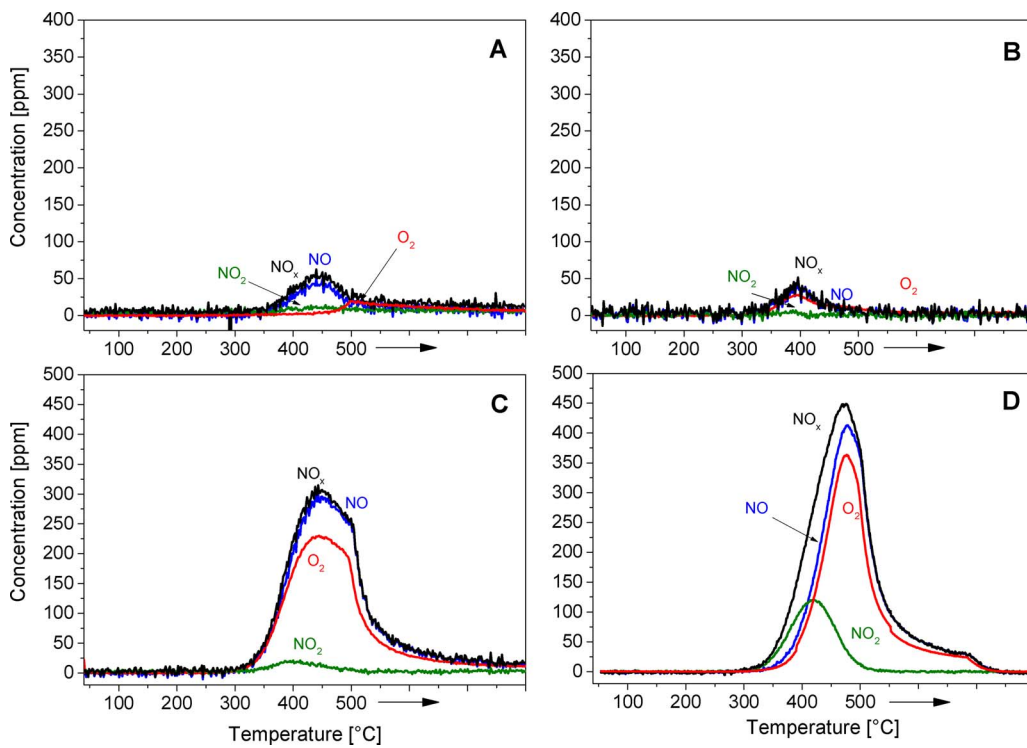


Fig. 12. Surface FT-IR analysis during thermal decomposition in inert atmosphere (TPD) of nitrite species stored onto A) Ba/Al<sub>2</sub>O<sub>3</sub>, B) Pt/Al<sub>2</sub>O<sub>3</sub>, C) Pt/Al<sub>2</sub>O<sub>3</sub> + Ba/Al<sub>2</sub>O<sub>3</sub> physical mixture. Storage conditions: 1000 ppm NO + 3% v/v O<sub>2</sub> in He at 150 °C; thermal decomposition in He from 50 to 500 °C (10 °C/min).



**Fig. 13.** Thermal decomposition in inert atmosphere (TPD) of nitrate species stored onto: A) Ba/Al<sub>2</sub>O<sub>3</sub>, B) Pt/Al<sub>2</sub>O<sub>3</sub>, C) Pt/Al<sub>2</sub>O<sub>3</sub> + Ba/Al<sub>2</sub>O<sub>3</sub> physical mixture, D) Pt-Ba/Al<sub>2</sub>O<sub>3</sub> catalyst surface. Storage conditions: 1000 ppm NO + 3% v/v O<sub>2</sub> in He at 350 °C; thermal decomposition in He from 50 to 500 °C (10 °C/min).

NO and nitrates.

The results obtained during the TPD run carried out over the Pt/Al<sub>2</sub>O<sub>3</sub> + Ba/Al<sub>2</sub>O<sub>3</sub> physical mixture after NO<sub>x</sub> adsorption at 150 °C are shown in Fig. 11C. A complex situation is apparent in the NO<sub>x</sub> evolution, with a first NO and NO<sub>2</sub> desorption peak in the low-temperature region with maximum near 215 °C; a second peak in the 300–400 °C temperature range where the evolution of NO, O<sub>2</sub> and NO<sub>2</sub> is observed; and finally a high temperature desorption peak (above 400 °C) corresponding to NO and O<sub>2</sub> evolution. We recall that in this case, due to the formation of small amounts of NO<sub>2</sub> over the Pt/Al<sub>2</sub>O<sub>3</sub> sample, the storage of nitrates over Ba/Al<sub>2</sub>O<sub>3</sub> is enhanced. Accordingly, a comparison of the results obtained in the case of the physical mixture with those shown in the inset of Fig. 11A (Ba/Al<sub>2</sub>O<sub>3</sub> upon adsorption of NO/NO<sub>2</sub> mixture) and in Fig. 11B (Pt/Al<sub>2</sub>O<sub>3</sub>) suggests that the TPD obtained with the physical mixture arise from the superposition of the TPD profiles of the individual Ba/Al<sub>2</sub>O<sub>3</sub> and Pt/Al<sub>2</sub>O<sub>3</sub> samples. This is supported by the FT-IR spectra shown in Fig. 12C where an initial decrease of the band at 1215 cm<sup>-1</sup>, associated to the presence of Al and Ba nitrates, is observed. Notably, the band also broadens with temperature, suggesting that nitrates stored on alumina sites (i.e. on the Pt/Al<sub>2</sub>O<sub>3</sub> particles, characterized by a sharper band) decompose at first, followed by the decomposition of nitrates on Ba sites. Above 300 °C, the formation of nitrate species (on alumina, band at 1565 cm<sup>-1</sup>) is also evident, due to the disproportion of nitrates on alumina (reaction (10)). Eventually at higher temperatures the nitrate species decompose and the related band observed at 1565 cm<sup>-1</sup> is eroded; however, nitrates are still present on physical mixture after desorption at 500 °C, along with nitrates on Ba sites. Hence, these data point out the absence of interactions in the decomposition pathways of the nitrate species stored over the individual Pt/Al<sub>2</sub>O<sub>3</sub> and Ba/Al<sub>2</sub>O<sub>3</sub> particles in the physical mixture.

Finally, in Fig. 11D the TPD profiles obtained in the case of nitrates stored over the Pt-Ba/Al<sub>2</sub>O<sub>3</sub> surface are shown [19,21]. The onset temperature for nitrate decomposition is observed near 125 °C; two NO desorption peaks are observed with maxima centered at 300 °C and 500 °C, this latter corresponding to the end of the heating ramp. The evolution of NO at high temperature is accompanied by that of O<sub>2</sub>,

whereas at low temperatures the desorption of small amounts of NO<sub>2</sub> are observed. These data, along with the calculated N/O ratio of the desorbing products (close to 1 at low temperatures and at 0.4 at high temperatures) can be explained by invoking the disproportion of nitrates stored over Ba to nitrates and NO, followed by nitrate decomposition (reaction (11)), according to the lines previously depicted for the Pt/Al<sub>2</sub>O<sub>3</sub> catalyst. This has also been confirmed by FT-IR data already discussed elsewhere [19].

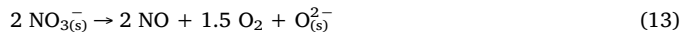
Therefore, the data show that nitrates stored over the Pt-containing samples (i.e. Pt/Al<sub>2</sub>O<sub>3</sub> and Pt-Ba/Al<sub>2</sub>O<sub>3</sub>) undergo a disproportion reaction. At variance, nitrates stored over Ba/Al<sub>2</sub>O<sub>3</sub> (either alone or in the physical mixture) decompose at higher temperatures without nitrate formation. This clearly points out the role of Pt in the nitrite disproportion reaction. It can be suggested that the reaction is occurring at the Pt/Ba or Pt/Al interface [19], where the thermal decomposition of nitrates initially leads to Pt-O species and to the production of gaseous NO. Pt-O species are then involved in the oxidation of nitrates to nitrates, and accordingly no net release of oxygen is observed in the gas phase at low temperature and nitrate species are formed. Accordingly, Pt plays a role in the decomposition of the stored nitrates and in the formation of nitrates as well. It is worth to note that the complete regeneration of the catalyst observed in the TPD experiments implies reverse spillover of NO<sub>x</sub> from BaO to Pt sites and is driven by the removal of oxygen atoms from Pt, in line with previous reports by Cant et al. [33]. At variance, in the absence of Pt (i.e. over Ba/Al<sub>2</sub>O<sub>3</sub>), nitrates decompose to gaseous species without disproportion to nitrates. In any case, the stored NO<sub>x</sub> species present a high thermal stability: this makes these systems unappropriate for PNA applications, where a much lower decomposition temperature is required to accomplish the release of the stored NO<sub>x</sub> in a suitable temperature range for SCR applications (in the range 200–250 °C).

The results of the TPD experiments carried out after NO<sub>x</sub> adsorption at 350 °C are shown in Fig. 13. In this case nitrates have been stored in the case of the Ba/Al<sub>2</sub>O<sub>3</sub> samples (Fig. 5B), and nitrates in the other cases (Figs. 5 A, 6 B and D).

In the case of the Ba/Al<sub>2</sub>O<sub>3</sub> sample (Fig. 13A), nitrates decomposition occurs according to the lines already described for the TPD after

adsorption at 150 °C, i.e. NO and O<sub>2</sub> evolution is seen although the poor oxygen desorption which is observed might be related to the formation of Ba peroxide species that release oxygen only at high temperatures.

In the case of Pt/Al<sub>2</sub>O<sub>3</sub> (Fig. 13B) the onset temperature for nitrate decomposition is observed near 350 °C, with evolution of NO as major decomposition product, accompanied by O<sub>2</sub> evolution. The decomposition of nitrates over Pt/Al<sub>2</sub>O<sub>3</sub> occurs according to stoichiometry of reaction (13), as confirmed by the calculated N/O ratio evolved during the TPD:



On the Ba/Al<sub>2</sub>O<sub>3</sub> – Pt/Al<sub>2</sub>O<sub>3</sub> physical mixture and Pt-Ba/Al<sub>2</sub>O<sub>3</sub> catalyst (Fig. 13C and D, respectively) the nitrates decomposition is observed starting from 325 °C; NO and O<sub>2</sub> represent the major decomposition products, with maxima centered near 450 °C and 475 °C in the case of physical mixture and Pt-Ba/Al<sub>2</sub>O<sub>3</sub> catalyst, respectively. Minor amounts of NO<sub>2</sub> are also detected in the case of the Pt-Ba/Al<sub>2</sub>O<sub>3</sub> catalyst, with maximum near 420 °C. In all cases, the calculated N/O ratio evolved during the TPD run is close to 0.4, consistent with the decomposition of nitrates. Notably, the NO peak observed in the case of the Pt-Ba/Al<sub>2</sub>O<sub>3</sub> catalyst is narrower if compared to that observed in the case of the physical mixture since in this case the peak originates from the superposition of the peaks related to the decomposition of nitrates stored on Pt/Al<sub>2</sub>O<sub>3</sub> and on Ba/Al<sub>2</sub>O<sub>3</sub>, having different thermal stability. Notably the nitrates stored over Ba in the Pt-Ba/Al<sub>2</sub>O<sub>3</sub> catalyst are decomposed at lower temperatures with respect to the Ba/Al<sub>2</sub>O<sub>3</sub> sample in view of the role of Pt in the nitrate decomposition, as already discussed elsewhere [19].

The role of water on the thermal decomposition of the NO<sub>x</sub> adsorbed species has been investigated by TPD experiments in the case of the Pt-Ba/Al<sub>2</sub>O<sub>3</sub> sample and of the Ba/Al<sub>2</sub>O<sub>3</sub> – Pt/Al<sub>2</sub>O<sub>3</sub> physical mixture, after NO/O<sub>2</sub> adsorption at 150 °C in the presence of 1% v/v of water. The TPD run has been carried out in the presence of water as well. The results indicated that water has a limited impact on the decomposition of the stored NO<sub>x</sub> species. This is shown in Fig. 14 in the case of the mechanical mixture, taken as example. In fact upon comparing Fig. 14 with Fig. 11C (TPD in the absence of water) it appears that the presence of water decreases the low-T desorption peak (thus suggesting that water inhibits the formation of the less stable nitrites), whereas the impact of water on the high-T peak seems of minor importance.

#### 3.4. Reactivity of the stored NO<sub>x</sub> species

The reactivity of the species stored at 150 °C (i.e. nitrites) towards H<sub>2</sub> as reducing agent has been investigated under isothermal conditions and the results of the gas phase and FT-IR analysis are reported in Fig. 15A and B, respectively, for the Pt-Ba/Al<sub>2</sub>O<sub>3</sub> catalyst and in

Fig. 15C and D for the physical mixture.

On the Pt-Ba/Al<sub>2</sub>O<sub>3</sub> catalyst, after H<sub>2</sub> admission to the reactor (t = 0 s), H<sub>2</sub> is completely consumed and N<sub>2</sub>, NH<sub>3</sub> and N<sub>2</sub>O are detected at the reactor outlet with different quantities. N<sub>2</sub>O is observed only during the initial stages of the reduction in small amounts (less than 80 ppm). After 220 s the H<sub>2</sub> breakthrough is observed and the NH<sub>3</sub> and N<sub>2</sub> concentration decrease. FT-IR spectra (Fig. 15B) show the progressive consumption of nitrates upon H<sub>2</sub> admission at 150 °C; after 15 min only small amounts of nitrates are still present on the catalyst surface.

The products evolution is in line with the reduction mechanisms proposed in the literature [34–38]. It is suggested that upon H<sub>2</sub> admission the noble metal sites become reduced. This leads to the reduction of the NO<sub>x</sub> species stored close-by to the Pt sites, leading to the release of NO. NO<sub>x</sub> species stored far away from Pt may spill over the support towards the reduced Pt sites [34,38], and therefore are also involved in the reduction. Released NO is then converted to N<sub>2</sub>O, N<sub>2</sub> and NH<sub>3</sub> depending on the oxidation state of Pt [39]. The so-formed N<sub>2</sub>O and N<sub>2</sub> exit the reactor and are detected during the initial part of the reduction, whereas ammonia may further react with NO<sub>x</sub> stored downstream of the H<sub>2</sub> front [34] leading to N<sub>2</sub> formation (reaction (14)):



However due to the poor reactivity of NH<sub>3</sub> towards the stored NO<sub>x</sub> at this temperature, significant amounts of unconverted NH<sub>3</sub> are emitted. This pathway efficiently removes the stored NO<sub>x</sub> since only minor amounts of nitrates remain adsorbed at the end of the reduction.

In the case of the Pt/Al<sub>2</sub>O<sub>3</sub> + Ba/Al<sub>2</sub>O<sub>3</sub> physical mixture (Fig. 15C), upon H<sub>2</sub> admission only N<sub>2</sub> (near 80 ppm) is immediately observed at the reactor outlet, before the H<sub>2</sub> breakthrough (100 s). Then, with a delay of 400 s, the concentration of ammonia starts to increase, showing a very broad peak with maximum near 60 ppm. Then the catalyst has been heated (starting from near 4000 s) and this led to complete the NO<sub>x</sub> reduction, as pointed out by the observed H<sub>2</sub> consumption and ammonia production. Fig. 15D shows the FT-IR spectra recorded during the parallel FT-IR experiment. In agreement with the gas phase analysis, nitrite reduction is not complete at 150 °C and it is necessary to increase the temperature up to 500 °C to have the complete reduction of nitrates. It is worth of note that nitrite band becomes broader on increasing the temperature: this suggests that nitrates stored on Al sites of the Pt/Al<sub>2</sub>O<sub>3</sub> particles are initially involved in the reduction at 150 °C, according to the pathways described above for the Pt-Ba/Al<sub>2</sub>O<sub>3</sub> sample. Then, upon temperature increase, nitrates stored on Ba/Al<sub>2</sub>O<sub>3</sub> particles are also reduced. However, in this case Ba-nitrates are thermally decomposed to gaseous NO, which in turn is reduced to ammonia over the Pt sites of Pt/Al<sub>2</sub>O<sub>3</sub>. This picture is consistent with

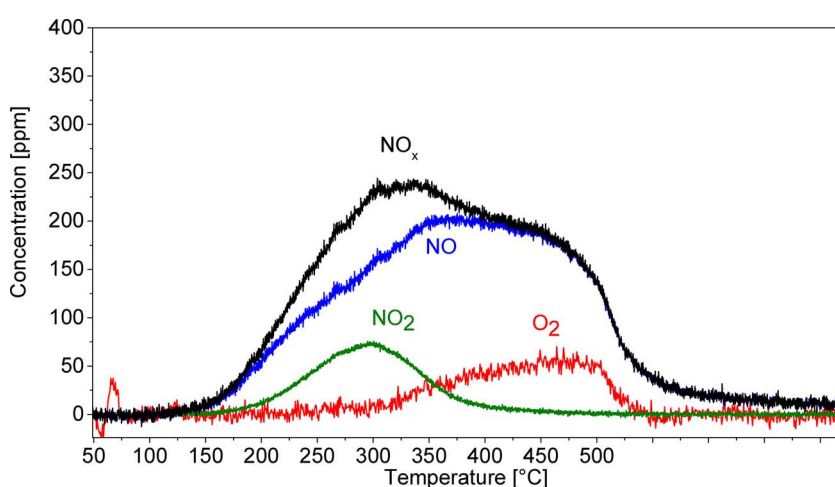
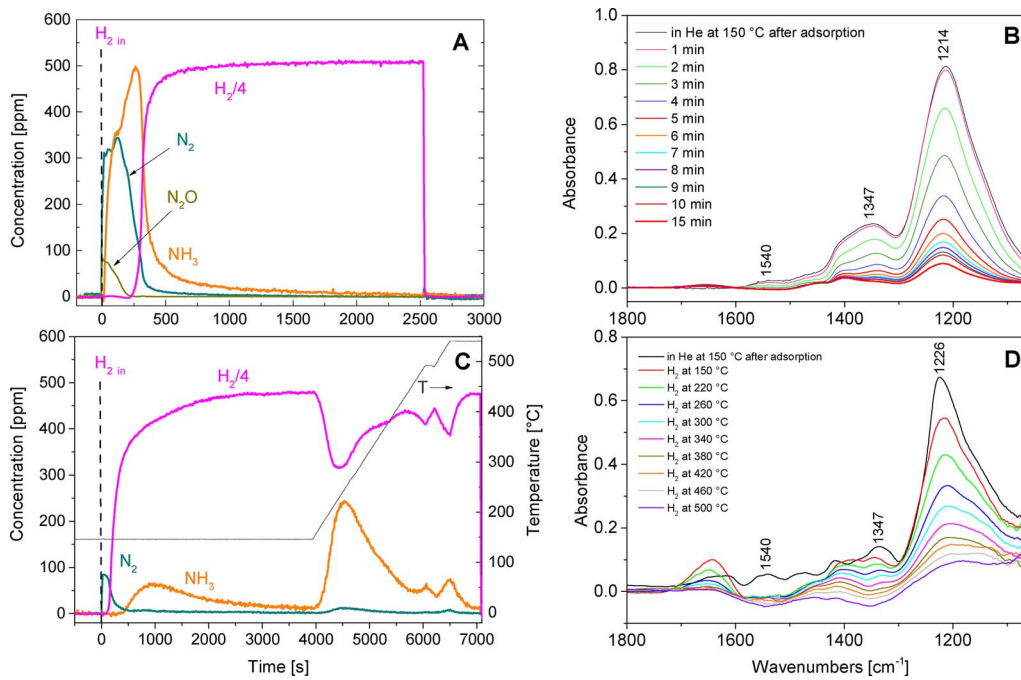


Fig. 14. Thermal decomposition (TPD) under He + 1% v/v H<sub>2</sub>O of nitrite species stored onto Pt/Al<sub>2</sub>O<sub>3</sub> + Ba/Al<sub>2</sub>O<sub>3</sub> physical mixture. Storage conditions: 1000 ppm NO + 3% v/v O<sub>2</sub> + 1% v/v H<sub>2</sub>O in He at 150 °C; thermal decomposition in He + 1% v/v H<sub>2</sub>O from 50 to 500 °C (10 °C/min).



the results obtained upon the reduction of nitrites stored over the individual Pt/Al<sub>2</sub>O<sub>3</sub> and Ba/Al<sub>2</sub>O<sub>3</sub> samples (data not shown), indicating that nitrites stored over Pt/Al<sub>2</sub>O<sub>3</sub> can be effectively reduced at 150 °C, whereas nitrites stored on Ba/Al<sub>2</sub>O<sub>3</sub> are hardly involved in the reduction process and decompose to NO/O<sub>2</sub> only at higher temperatures upon heating. Accordingly, the data indicate that only the NO<sub>x</sub> species stored on adsorption sites present on the same catalyst particle with Pt (e.g. in the case of the Pt-Ba/Al<sub>2</sub>O<sub>3</sub> ternary catalyst) can be involved in the reduction process. Notably, the NO<sub>x</sub> species stored onto the Ba/Al<sub>2</sub>O<sub>3</sub> sample of the physical mixture could not be reduced in spite of the fact that H<sub>2</sub> activated over Pt/Al<sub>2</sub>O<sub>3</sub> could migrate to the Ba/Al<sub>2</sub>O<sub>3</sub> particles [19]. Hence this suggests that the reduction occurs upon migration of the adsorbed NO<sub>x</sub> species towards Pt, and that the inter-particle spillover of the stored NO<sub>x</sub> species is not an effective pathway. In fact, on the physical mixture, NO<sub>x</sub> adsorbed over Ba could be removed only upon thermal decomposition at high temperatures.

Finally, the reactivity with H<sub>2</sub> of nitrates stored at 350 °C has also been investigated and the results are shown in Fig. 16A, B for the ternary Pt-Ba/Al<sub>2</sub>O<sub>3</sub> catalyst, and in Fig. 16C, D for the Pt/Al<sub>2</sub>O<sub>3</sub> + Ba/Al<sub>2</sub>O<sub>3</sub> physical mixture. In the case of Pt-Ba/Al<sub>2</sub>O<sub>3</sub> catalyst, upon H<sub>2</sub> addition to the reactor (t = 0 s) H<sub>2</sub> is completely consumed while the N<sub>2</sub> outlet concentration increases immediately to a level near 400 ppm [8,34] (Fig. 16A). Then, in correspondence to H<sub>2</sub> breakthrough (300 s), the N<sub>2</sub> concentration decreases and the evolution of NH<sub>3</sub> occurs. The FT-IR spectra recorded during the isothermal reduction (Fig. 16B) show the very fast reduction of nitrate bands intensity that are almost completely removed after 5 min. No other surface species have been observed. As previously discussed in the case of nitrites reduction, the observed product distribution can be explained on the basis of the reduction of nitrates with H<sub>2</sub> to give NH<sub>3</sub>, followed by the reaction of NH<sub>3</sub> with the stored nitrates to form N<sub>2</sub> [34]. At 350 °C the reaction is more selective towards N<sub>2</sub> in view of the higher reactivity of ammonia towards stored nitrates [34,39].

Finally, the reduction of nitrates stored over the physical mixture is shown in Fig. 16C. In this case an initial total consumption of H<sub>2</sub> is observed, accompanied by the production of N<sub>2</sub> at first and of NH<sub>3</sub> later on (delay near 100 s). FT-IR spectra (Fig. 16D) indicate that this initial product formation corresponds to the reduction of nitrates stored on Al sites of Pt/Al<sub>2</sub>O<sub>3</sub> particles (bands at 1565 cm<sup>-1</sup> and 1300 cm<sup>-1</sup>). Bands at 1320 cm<sup>-1</sup> and at 1408 cm<sup>-1</sup>, corresponding to nitrates stored over

**Fig. 15.** Reactivity under isothermal conditions of nitrites species stored onto A, B) Pt-Ba/Al<sub>2</sub>O<sub>3</sub>, C, D) Pt/Al<sub>2</sub>O<sub>3</sub> + Ba/Al<sub>2</sub>O<sub>3</sub> physical mixture. A, C gas phase analysis; B, D FT-IR spectra. Storage conditions: 1000 ppm NO + 3% v/v O<sub>2</sub> in He at 150 °C; reduction: 2000 ppm H<sub>2</sub> in He at 150 °C.

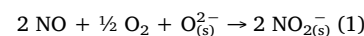
Ba sites of Ba/Al<sub>2</sub>O<sub>3</sub> particles, are not affected, indicating that these species cannot be reduced at this temperature. However, they are removed upon heating at 500 °C, that provokes the thermal decomposition of the nitrates stored on Ba leading to the evolution of gas-phase NO which in turn is reduced by H<sub>2</sub> to NH<sub>3</sub> (see Fig. 16C) over Pt/Al<sub>2</sub>O<sub>3</sub>.

Finally, as already discussed in other papers from our group, it is worth to be mentioned that water has a slightly beneficial effect on the reduction of stored NO<sub>x</sub>, possibly because it increases the mobility of the NO<sub>x</sub> surface species and/or the H<sub>2</sub> spillover [40]. At variance, CO<sub>2</sub> has an inhibiting effect due to poisoning of Pt by CO formed upon the reverse water gas-shift reaction [38].

#### 4. Conclusive remarks

In this study mechanistic aspects related to the adsorption of NO<sub>x</sub> over alumina-supported Pt, Ba and PtBa catalysts have been deepened. In particular, the role of NO/NO<sub>2</sub> and of the various catalyst components in the storage of NO<sub>x</sub> has been disclosed. The thermal decomposition and reactivity with H<sub>2</sub> of the adsorbed species have been addressed as well, and new insights on the pathways involved in the adsorption of NO<sub>x</sub> over various surfaces and on their decomposition and reactivity have been eventually obtained.

At 150 °C, nitrites are formed on all surfaces when starting from NO/O<sub>2</sub>. Nitrites are formed through different routes. A pathway involves the interaction of NO/O<sub>2</sub> with O<sub>(s)</sub><sup>2-</sup> surface oxygen anion, e.g. lattice oxygen of Ba sites in the case of the Ba containing samples and oxygen species of the alumina support in the case of the Ba-free samples, i.e. reaction (1):



The nature of the formed nitrite species is different due to the different basicity of the adsorption sites (Al vs. Ba sites); these species can be distinguished spectroscopically. Pt favors the nitrite formation being involved in the activation of O<sub>2</sub>/NO molecules and hence providing the required oxygen anions to the storage sites. In particular, when Pt and Ba are in close proximity, like in the Pt-Ba/Al<sub>2</sub>O<sub>3</sub> sample, the NO<sub>x</sub> adsorption is enhanced due to the cooperative effect between the Ba storage sites and the Pt oxidation sites. Notably, significant amounts of nitrites are stored in spite of the very poor NO to NO<sub>2</sub> oxidation. This clearly points out that the NO oxidation to NO<sub>2</sub> is not required to store

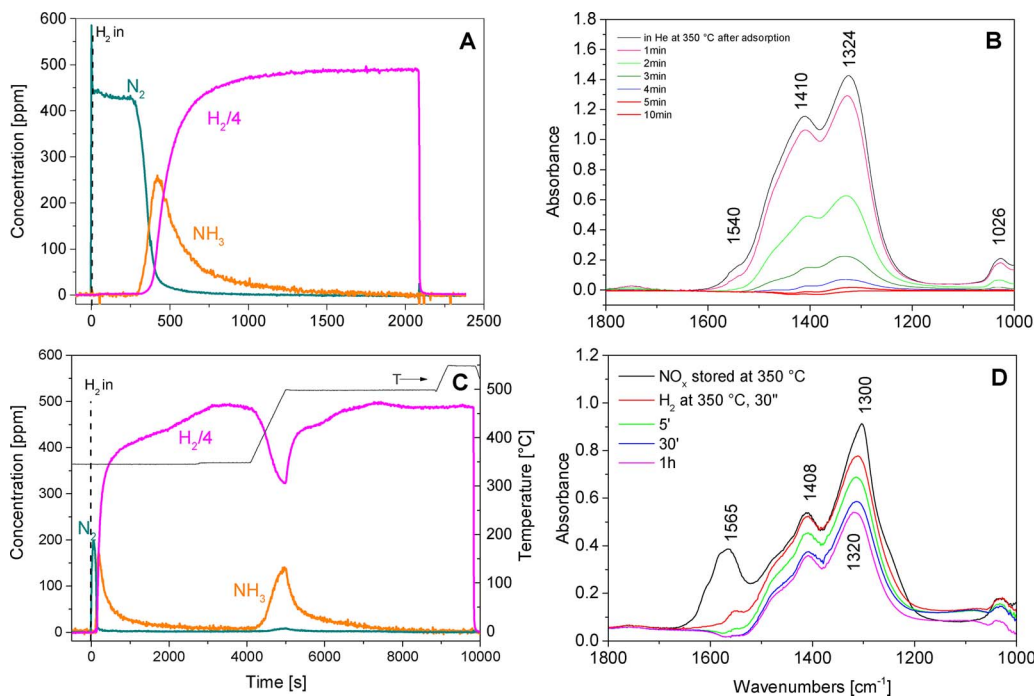


**Fig. 16.** Reactivity under isothermal conditions of nitrates species stored onto A, B) Pt-Ba/Al<sub>2</sub>O<sub>3</sub>, C, D) Pt/Al<sub>2</sub>O<sub>3</sub> + Ba/Al<sub>2</sub>O<sub>3</sub> physical mixture. A, C: gas phase analysis; B, D: FT-IR spectra. Storage conditions: 1000 ppm NO + 3% v/v O<sub>2</sub> in He at 350 °C; reduction: 2000 ppm H<sub>2</sub> in He at 350 °C.

nitrates on the surface.

Pt also promotes the oxidation of NO to NO<sub>2</sub>, and this provides an additional route for the storage of nitrates involving the vicinal co-adsorption of NO and NO<sub>2</sub> via the following reaction:



This route is in fact exploited in the Pt/Al<sub>2</sub>O<sub>3</sub> + Ba/Al<sub>2</sub>O<sub>3</sub> physical mixture where the Ba/Al<sub>2</sub>O<sub>3</sub> component is able to store more nitrates than the bare Ba/Al<sub>2</sub>O<sub>3</sub> sample, due to the presence of small amounts of NO<sub>2</sub> formed onto the Pt/Al<sub>2</sub>O<sub>3</sub> sample. Accordingly, this points out to the existence of a synergistic effect in the NO<sub>x</sub> storage between the Pt/Al<sub>2</sub>O<sub>3</sub> and Ba/Al<sub>2</sub>O<sub>3</sub> components in the physical mixture, occurring via the gas-phase migration of NO<sub>2</sub>. This route is however less efficient than the nitrite storage over Pt-Ba/Al<sub>2</sub>O<sub>3</sub>, indicating that i) reaction (1) is more important than reaction (2) in the storage of nitrates; and ii) the NO<sub>x</sub> storage according to reaction (1) is enhanced when the Ba storage sites and Pt are in close proximity. In fact, over Pt-Ba/Al<sub>2</sub>O<sub>3</sub> the storage of NO to nitrates is much faster than the oxidation of NO to NO<sub>2</sub>.

When the NO<sub>x</sub> storage is carried out at higher temperatures (350 °C), nitrates have always been observed at the early stages of adsorption. However, in the presence of Pt, nitrite species rapidly disappear being transformed into nitrate species. At such high temperatures both the formation of nitrates and the oxidation of nitrites into nitrates is accomplished by NO<sub>2</sub>, formed upon NO oxidation. In fact, direct evidence has been provided in this work that NO<sub>2</sub> may participate both in the formation of nitrites/nitrates adspecies following the stoichiometry of the following disproportion reaction (4):



and in the oxidation of nitrites to nitrates as well, reaction (6):



In fact, where NO<sub>2</sub> is not detected (e.g. over the Ba/Al<sub>2</sub>O<sub>3</sub> catalyst) nitrates are formed on the catalyst surface and are not oxidized to nitrates even at high temperatures. At variance, nitrates formed over the same Ba/Al<sub>2</sub>O<sub>3</sub> sample in the physical mixture are readily transformed into nitrates by NO<sub>2</sub> formed over the Pt/Al<sub>2</sub>O<sub>3</sub> component.

The discussed pathways for NO<sub>x</sub> storage hold in the presence of water and CO<sub>2</sub> as well. In the presence of such species the Ba storage

sites are in the form of hydroxide and/or carbonates: however the NO<sub>x</sub> storage is not greatly affected being Ba hydroxide/carbonate species displaced by the nitrates/nitrates.

The thermal decomposition of the adsorbed NO<sub>x</sub> species has also been investigated. In all cases nitrates decompose to NO/O<sub>2</sub> (and minor amounts of NO<sub>2</sub>) when heated above the adsorption temperature. However, the nitrates stored over Ba in the Pt-Ba/Al<sub>2</sub>O<sub>3</sub> catalyst are decomposed at lower temperatures with respect to the species adsorbed onto the Ba/Al<sub>2</sub>O<sub>3</sub> sample (either alone or in the mechanical mixture), pointing out the role of Pt in the nitrate decomposition.

Along similar lines, nitrites adsorbed over Ba/Al<sub>2</sub>O<sub>3</sub> at both 150 and 350 °C decompose to NO/NO<sub>2</sub>/O<sub>2</sub>. At variance, in the presence of Pt (i.e. Pt/Al<sub>2</sub>O<sub>3</sub> and Pt-Ba/Al<sub>2</sub>O<sub>3</sub> samples) nitrites decomposition results in a complex pathway showing the initial evolution of NO and in the simultaneous formation of nitrates, according to the following disproportion reaction of nitrites (10):



Eventually nitrates decompose at high temperatures into NO and O<sub>2</sub>. Hence the results point out that Pt has a direct role in the decomposition of the adsorbed species, catalyzing the occurrence of the nitrite disproportion reaction. In any case, the stored NO<sub>x</sub> species present a high thermal stability: this makes these systems unappropriate for PNA applications, where a much lower decomposition temperature is required to accomplish the release of the stored NO<sub>x</sub> in a suitable temperature range.

Finally, the reactivity of the NO<sub>x</sub> stored species towards H<sub>2</sub> has also been investigated. Only the NO<sub>x</sub> species stored on the Pt-Ba/Al<sub>2</sub>O<sub>3</sub> catalyst and on the Pt/Al<sub>2</sub>O<sub>3</sub> catalyst could be reduced at temperatures well below that of adsorption. On the other hand, the NO<sub>x</sub> species stored on the Ba/Al<sub>2</sub>O<sub>3</sub> catalyst of the physical mixture could be reduced only above the decomposition temperature. In fact, in such a case the stored NO<sub>x</sub> decompose to gaseous species that are then reduced over the Pt/Al<sub>2</sub>O<sub>3</sub> sample, as clearly proved by FT-IR data. Accordingly, the data indicate that only the NO<sub>x</sub> species stored on adsorption sites in close proximity with Pt can be involved in the reduction process, in spite of the fact that H<sub>2</sub> activated over Pt/Al<sub>2</sub>O<sub>3</sub> could migrate to the Ba/Al<sub>2</sub>O<sub>3</sub> particles. Therefore, this also suggests that the reduction occurs upon migration of the adsorbed NO<sub>x</sub> species towards Pt, and that

the inter-particle spillover of the stored NO<sub>x</sub> species is not effective.

## References

- [1] <http://www.eea.europa.eu/>.
- [2] W.S. Epling, L.E. Campbell, A. Yezerets, N.W. Currier, J.E. Parks, *Catal. Rev.* 46 (2004) 163–245.
- [3] S. Roy, A. Baiker, *Chem. Rev.* 109 (2009) 4054–4409.
- [4] J.R. Theis, C.K. Lambert, *Catal. Today* 258 (2015) 367–377.
- [5] P. Forzatti, L. Lietti, I. Nova, E. Tronconi, *Catal. Today* 151 (2010) 202–211.
- [6] N. Takahashi, H. Shinjoh, T. Suzuki, K. Yamazaki, K. Yokota, H. Suzuki, N. Miyoshi, S. Matsumoto, T. Tanizawa, T. Tanaka, S. Tateishi, K. Kasahara, *Catal. Today* 27 (1996) 63–69.
- [7] S.I. Matsumoto, *Catal. Today* 90 (2004) 183–190.
- [8] P. Forzatti, L. Lietti, L. Castoldi, *Catal. Lett.* 145 (2015) 483–504.
- [9] L. Castoldi, R. Bonzi, L. Lietti, P. Forzatti, S. Morandi, G. Ghiootti, S. Dzwigaj, *J. Catal.* 282 (2011) 128–144.
- [10] J.R. Theis, E. Gulari, SAE Technical Paper 2006-01-0210 (2006).
- [11] D. Chatterjee, P. Kočí, V. Schmeïßer, M. Marek, M. Weibel, B. Krutzsch, *Catal. Today* 151 (2010) 395–409.
- [12] Y. Ji, Y. Bai, M. Crocker, *Appl. Catal. B* 170–171 (2015) 283–292.
- [13] J.E. Melville, R.J. Brisley, O. Keane, P.R. Phillips, E.H. Mountstevens, U.S. Patent 8105,559 (2012).
- [14] C.K. Koch, G., Qi, S.J., Schmieg, W. Li, U.S. Patent 2013/0294990 A1 (2013).
- [15] S. Tamm, S. Andonova, L. Olsson, *Catal. Lett.* 144 (2014) 674–684.
- [16] Y. Ji, V. Easterling, U. Graham, C. Fisk, M. Crocker, J.-S. Choi, *Appl. Catal. B* 103 (2011) 413–427.
- [17] S. Benramdhane, C.-N. Millet, E. Jeudy, J. Lavy, V. Blasin Aubè, M. Daturi, *Catal. Today* 176 (2011) 56–62.
- [18] N. Miyoshi, T. Tanizawa, K. Kasahara, S. Tateishi, European Patent Application 0669 157 A1 (1995).
- [19] L. Castoldi, L. Righini, R. Matarrese, L. Lietti, P. Forzatti, *J. Catal.* 328 (2015) 270–279.
- [20] L. Castoldi, I. Nova, L. Lietti, P. Forzatti, *Catal. Today* 96 (2004) 43–52.
- [21] A. Infantes-Molina, L. Righini, L. Castoldi, C.V. Loricera, J.L.G. Fierro, A. Sin, L. Lietti, *Catal. Today* 197 (2012) 178–189.
- [22] L. Lietti, M. Daturi, V. Blasin-Aubè, G. Ghiootti, F. Prinetto, P. Forzatti, *Chem. Cat. Chem.* 4 (2012) 55–58.
- [23] L. Castoldi, L. Lietti, I. Nova, R. Matarrese, P. Forzatti, F. Vindigni, S. Morandi, F. Prinetto, G. Ghiootti, *Chem. Eng. J.* 161 (2010) 416–423.
- [24] S. Morandi, F. Prinetto, G. Ghiootti, L. Castoldi, L. Lietti, P. Forzatti, M. Daturi, V. Blasin-Aubè, *Catal. Today* 231 (2014) 116–124.
- [25] F. Prinetto, G. Ghiootti, I. Nova, L. Lietti, E. Tronconi, P. Forzatti, *J. Phys. Chem. B* 105 (2001) 12732–12745.
- [26] B.M. Weiss, K.B. Caldwell, E. Iglesia, *J. Phys. Chem. C* 115 (2011) 6561–6570.
- [27] N. Maeda, A. Urakawa, A. Baiker, *Top. Catal.* 52 (2009) 1746–1751.
- [28] U. Elizundia, R. López-Fonseca, I. Landa, M.A. Gutiérrez-Ortiz, J.R. González-Velasco, *Top. Catal.* 42–43 (2007) 37–41.
- [29] S.S. Chaugule, A. Yezerets, N.W. Currier, F.H. Ribeiro, W.N. Delgass, *Catal. Today* 151 (2010) 291–303.
- [30] L. Lietti, I. Nova, P. Forzatti, E. Tronconi, *J. Catal.* 204 (2001) 175–191.
- [31] S. Morandi, F. Prinetto, L. Castoldi, L. Lietti, P. Forzatti, G. Ghiootti, *Phys. Chem. Chem. Phys.* 15 (2013) 13409.
- [32] J. Szanyi, J.H. Kwak, D.H. Kim, X. Wang, R. Chimentao, J. Hanson, W.S. Epling, C.H.F. Peden, *J. Phys. Chem. C* 111 (2007) 4678.
- [33] N.W. Cant, M.J. Patterson, *Catal. Lett.* 85 (2003) 153–157.
- [34] I. Nova, L. Lietti, L. Castoldi, E. Tronconi, P. Forzatti, *J. Catal.* 239 (2006) 244–254.
- [35] R.D. Clayton, M.P. Harold, V. Balakotaiah, *AIChE J.* 55 (2009) 687–699.
- [36] V. Medhekar, V. Balakotaiah, M.P. Harold, *Catal. Today* 121 (2007) 226–236.
- [37] K.S. Kabin, P. Khanna, R.L. Muncrief, V. Medhekar, M.P. Harold, *Catal. Today* 114 (2006) 72–85.
- [38] R.D. Clayton, M.P. Harold, V. Balakotaiah, C.Z. Wan, *Appl. Catal. B* 90 (2009) 662–676.
- [39] L. Kubiak, R. Matarrese, L. Castoldi, L. Lietti, M. Daturi, P. Forzatti, *Catalysts* 6 (2016) 36.
- [40] L. Lietti, I. Nova, P. Forzatti, *J. Catal.* 257 (2008) 270–282.